LEPS/RCNP proposal

Photoproduction Experiment with Polarized HD Target at SPring-8

Organization

Name	Affrication	Position
M. Fujiwara	RCNP, Osaka Univ. and JAERI	Associate Professor/Group Leader
T. Hotta	RCNP, Osaka Univ.	Research Associate
H. Kohri	RCNP, Osaka Univ.	Post-Doctoral Fellow
T. Nakano	RCNP, Osaka Univ.	Professor
H. Fujimura	RCNP, Osaka Univ.	Researcher
M. Sumihama	RCNP, Osaka Univ.	Post-Doctoral Fellow
T. Matsumura	RCNP, Osaka Univ	Doctor Student
C. Commeaux	IN2P3, ORSAY	Researcher
J.-P. Didelez	IN2P3, ORSAY	Chief Researcher
G. Rouille	IN2P3, ORSAY	Researcher
M. Guidal	IN2P3, ORSAY	Researcher
N. Muramatsu	JAERI	Post-Doctoral Fellow
A. Titov	JINR, Dubna / JAERI	Prof. / Guest Research Scientist
A. Sakaguchi	Osaka Univ.	Associate Professor
T. Kishimoto	Osaka Univ.	Professor
S. Ajimura	Osaka Univ.	Research Associate
Y. Shimizu	Osaka Univ.	Researcher
S. Minami	Osaka Univ.	Doctor Student
T. Itabashi	Osaka Univ.	Doctor Student
J.K. Ahn	Pusan National Univ.	Associate Professor
M. Tanaka	Tokiwa Jr. Univ.	Professor
K. Hicks	Ohio Univ.	Professor

Contact address of spokesperson

M. Fujiwara
Research Center for Nuclear Physics, Osaka University
Mihogaoaka 10–1, Ibraki 567–0047, Osaka Japan
Phone: +81–6–6879–8914, FAX: +81–6–6879–8899
E-mail: fujiwara@rcnp.osaka-u.ac.jp

Contents

LEPS/RCNP proposal

Photoproduction Experiment with Polarized HD Target at SPring-8

M. Fujiwara, T. Hotta, H. Kohri, T. Nakano, H. Fujimura, M. Sumihama, T. Matsumura
Research Center for Nuclear Physics, Osaka University, Ibaraki, Osaka 567-0047, Japan

J-P. Didelez, C. Commeaux, G. Rouille, M. Guidal
IN2P3, Institut de Physique Nucléaire, Orsay, France

M. Tanaka
Kobe Tokiwa Junior College, Ohtani-cho 2-6-2, Nagata, Kobe 653, Japan

J.K. Ahn
Department of Physics, Pusan National University, Pusan 609-735, Korea

K. Hicks
Department of Physics, Ohio University, Athens, Ohio 45701, USA

N. Muramatsu, A. Titov
Advanced Science Research Center, Japan Atomic Energy Research Institute (JAERI), Tokai, Ibaraki 319-1195, Japan

A. Sakaguchi, T. Kishimoto, S. Ajimura, Y. Shimizu, S. Minami, T. Itabashi
Department of Physics, Osaka University, Toyonaka, Osaka 560-0043, Japan

Abstract

Measurement of double polarization asymmetries for ϕ photoproduction with the polarized target and a polarized photon beam is a sensitive means to investigate small and exotic amplitudes, such as an $s\bar{s}$-quark content of nucleons, via interferences with dominant amplitudes. The LEPS facility is suitable for this purpose because the experimental asymmetry is expected to be large at forward angles and in the LEPS energy region. In order to realize the double polarization measurements to study the $s\bar{s}$-quark content as well as exotic hadron structures, we propose to construct a frozen-spin polarized HD target for ϕ-meson photoproduction experiments at LEPS facility on the new basis of recent technology developments in cryogenic and high magnetic field. The solid HD target is ideal for a polarized target which is accessible to study photoreactions both on proton and deuteron with low background contributions. Polarization of H and D, which can be independently controlled, have already reached at 90% and 50%, respectively. Relaxation times for H and D polarizations reached at one week and one month, respectively. We estimate that a total cost for the construction of the HD target is about 3 million

US dollars. The construction will be completed within 4 years, and the associated experiment for ϕ-meson photoproduction will be performed in 10 days (40days) with the result of 20 % (10 %) accuracy for the double polarization asymmetry measurement.

1 Introduction

A high energy polarized photon beam produced by laser-induced backward Compton scattering (BCS) off electrons circulating in the storage ring is utilized for nuclear physics experiments at several synchrotron radiation facilities. Among the BCS photon facilities, the Laser Electron Photon beamline at SPring-8 (LEPS) produces the highest energy photon beam, and becomes a unique BCS facility in the world to have the ϕ photoproduction experiments, in combination with the measurements of polarization observables.

Measurement of polarization observables is very important for investigating the nature of hadron structures and the associated reaction mechanisms, because we can access the small amplitudes which are hardly seen in unpolarized cross sections. Sometimes, they are also very sensitive to the model description of the processes. The LEPS experiment started in December 2000 with an unpolarized liquid H_2 target and the linearly polarized photon beam. Some new results of ϕ and K^+ photoproduction have demonstrated the powerfulness of the polarization measurement at LEPS, and provided us a strong motivation for new experiments with a polarized target.

Photons produced in the BCS process are automatically highly polarized. However, the fabrication and installation of polarized targets require the very sophisticated and high technology. In this proposal, we review the scientific motivation to construct the Hydrogen-Deuterium polarized target called "HD target" and show the road-map to prepare the successful HD target at SPring-8.

In Section 2, we discuss the scientific motivations for the measurements of the photoreaction with polarized γ-rays and polarized targets. In Section 3, a brief explanation of the HD target and the present status of the development of the HD target at IPN-ORSAY are given. In Section 4 and 5, we review the existing LEPS facility and recent results with unpolarized target. Experimental consideration is discussed in Section 6. The costs and schedule for the experiment with polarized HD target are described in Section 7 and 8. A summary is presented in Section 9.

2 Scientific motivations

It is generally accepted that the low-energy properties of nucleon is well described in terms of three constituent u and d quarks. The constituent quark model predicts that the ratio (μ_n/μ_p) of the neutron and proton magnetic moments is $-2/3$, which agrees with the experimental value -0.685. However, the recent experiments from the lepton deep inelastic scattering address a serious question; the magnetic moments from constituent quarks only contribute 10%. Measurements of the nucleon spin structure functions indicate that there may be non-negligible strange quark content and that the strange quarks give $10-20\%$

contributions to the nucleon spin [1, 2, 3]. A similar conclusion has been drawn from the elastic νp scattering at BNL [4]. Analysis of the pion nucleon sigma term also suggest that proton might contain an admixture of 20% strange quarks [5, 6]. Experiments on annihilation reactions $p\bar{p} \rightarrow \phi X$ at rest [7, 8, 9] show a strong violation of the OZI rule [10]. However, it has also been argued that such experimental results could be understood with little or no strangeness content in the nucleon. These experimental as well as theoretical situations remain the $s\bar{s}$ content of nucleon as a long-standing problem in physics. Thus, this controversy should be solved by providing new experimental information on the $s\bar{s}$ content of nucleon.

The ϕ photoproduction is one of the promising reactions to give direct experimental data for studying the $s\bar{s}$ contents of nucleon. The ϕ meson has the pure $s\bar{s}$ wave function. Thus, there is a possibility of pinning down the $s\bar{s}$ components in a nucleon through the knockout process, where the $s\bar{s}$ pair couples to the photon and is knocked out as a ϕ meson. Although the $s\bar{s}$ knockout amplitude is much smaller than that from the dominant Pomeron exchange process in the ϕ meson photoproduction, it is predicted that double polarization asymmetries with a polarized proton target and a polarized beam are sensitive to the $s\bar{s}$ content via an interference effect. Theoretical calculations suggest that the effect of the $s\bar{s}$ content is detectable via beam-target asymmetry C_{BT} (defined in this section below) measurements at $E_\gamma \sim 2$ GeV, and that the LEPS energy region ($E_\gamma = 1.5 \sim 2.4$ GeV) is suitable to perform the C_{BT} measurement (Fig. 6.).

2.1 Spin observables in ϕ photoproduction

In this section, we discuss several topics related to the beam-target asymmetry in ϕ-meson photoproduction as a tool for studying hidden strangeness in a nucleon and other exotic channels with circularly polarized photon beam and polarized target.

2.1.1 Main processes in ϕ-meson photoproduction

The conventional ϕ-meson photoproduction amplitude is defined by the several "elementary" processes. Fig.1 shows the Fyenman diagrams associating with ϕ-meson photoproductions. The detailed discussions are given in Refs.[11, 12]. The "diffractive" - photoproduction amplitude is dominated by the Pomeron-exchange process in a wide energy range. This diffractive process is shown in Fig. 1(a). In this process, a photon changes to a vector meson, which is scattered in the multi-gluon exchange process. In the theoretical calculations, the glueball and scalar meson trajectories are included. The next channel is the pseudoscalar π and η-meson exchange. This process is relatively well defined in the theoretical analysis of the decay branching ratio from ϕ meson to $\rho\pi$ and $\eta\gamma$. Detailed experimental study of these contributions is underway at LEPS with unpolarized target

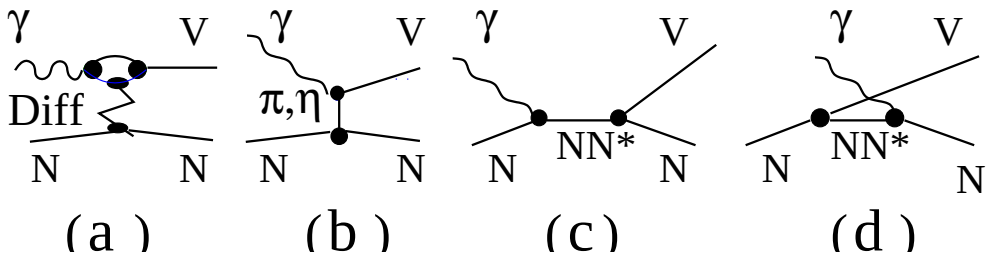

Figure 1: Diagrammatic representation of vector meson photoproduction from nucleon: (a) diffractive photoproduction, (b) pseudoscalar π and η-meson exchange and (c) direct and (d) crossed N and N^* exchanged processes.

and linearly polarized beam. At large momentum transfers, the dominant contribution comes from the nucleon and resonance excitation channels. The amplitudes of these channels are now well understood by the combined study of ω and ϕ-meson photoproduction at backward angles.

In addition to the conventional mechanisms mentioned above, the other more "exotic" processes may participate in ϕ-meson photoproduction amplitudes. Thus, the ϕ-meson photoproduction is an attractive and promising tool for studying the hidden component of "strangeness" in a nucleon [13, 14, 15]. The typical $s\bar{s}$-knockout processes, where the ϕ-meson is produced through direct interaction of incoming photon and $s\bar{s}$-component in a nucleon, is schematically shown in Fig. 2. The contribution of this channel at $E_\gamma = 2.2$

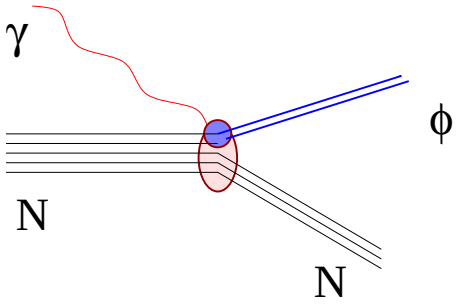

Figure 2: Diagrammatic representation of the $s\bar{s}$-knockout processes.

GeV to the total cross section is compared with the experimental data in Fig. 3 together with those of the other channels. One can see that the contribution of the $s\bar{s}$-knockout process is an order of magnitude smaller than those of the dominant diffractive channel. This means that an experimental study to measure spin observables, especially the beam-target asymmetry, is only the most promising candidate for revealing the nature of the $s\bar{s}$ content of a nucleon.

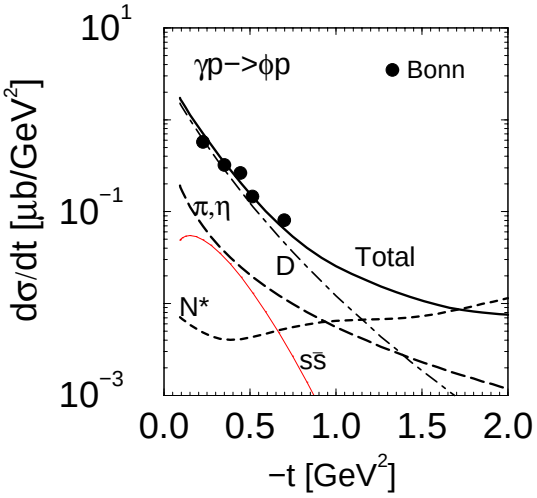

Figure 3: Differential cross sections of the $\gamma p \to \phi p$ reaction as a function of $-t$ at $E_\gamma = 2.2$ GeV. The experimental data are compared with the results of the theoretical calculations from the contributions of the diffractive channel (dot-dashed), the pseudoscalar-meson exchange (long dashed), the resonance excitation (dashed), $s\bar{s}$ (thin solid) and the full amplitude (thick solid). Data are taken from Ref. [17].

2.1.2 Beam-target asymmetry and $s\bar{s}$-knockout from a proton

Importance of the beam-target asymmetry in studying the $s\bar{s}$-knockout process can be understood by examining the spin structure of the photoproduction amplitude. The elementary amplitudes of the photoproduction processes (diffractive channel, pseudoscalar meson exchange, $s\bar{s}$-knockout) at forward angles (see Figs. 1 and 2.) have the following spin-conserving properties

$$\lambda_\gamma + m_i = \lambda_\phi + m_f \tag{1}$$

$$\lambda_\gamma = \lambda_\phi, \qquad m_i = m_f, \tag{2}$$

where λ_γ, λ_ϕ, m_i, m_f are the helicities of the photon, ϕ-meson, and the proton spin projections in the initial and final states, respectively. One can see that together with the total spin conservation (Eq. 1), those processes appear under the condition keeping the spin/helicity conservation in fermion and boson sectors, separately (Eq. 2). All of them can be divided into processes with natural-parity T^N ("electric-type") and unnatural-parity T^U ("magnetic-type") transitions

$$T^{\mathrm{N(U)}}_{m_f m_i;\lambda_V \lambda_\gamma}(t) = \begin{pmatrix} 1 \\ 2 m_i \lambda_\gamma \end{pmatrix} \delta_{m_f m_i} \delta_{\lambda_\gamma \lambda_V} T_0^{\mathrm{N(U)}}(t), \tag{3}$$

where $T_0^{N(U)}$ is the spin-independent part of the amplitude. The diffractive and pseudoscalar exchange amplitudes have the natural and unnatural parity-exchange property,

respectively. The parity-property of the $s\bar{s}$-knockout amplitude depends on the type of the elementary transition of γ+$s\bar{s}\rightarrow\ \phi$. The elementary spin-flip processes, like $^1S\rightarrow\ \phi$, result in unnatural parity-exchange amplitude. Following Ref. [13], it is assumed that the half of the $s\bar{s}$ configurations contributes to the unnatural parity-exchange process.

Eq. (3) shows that the unnatural parity exchange amplitude changes its phase following the sign of the photon helicity (at fixed target polarization): $\lambda_\gamma,\ m_i \rightarrow -\lambda_\gamma,\ m_i$, whereas the phase of the natural-parity exchange amplitude remains unchanged. This phase dependence plays a key role in the measurement of the beam-target asymmetry defined as

$$C_{BT} = \frac{d\sigma(\binom{\rightarrow}{\rightarrow}) - d\sigma(\binom{\leftarrow}{\rightarrow})}{d\sigma(\binom{\rightarrow}{\rightarrow}) + d\sigma(\binom{\leftarrow}{\rightarrow})}, \tag{4}$$

where the arrows represent the spin projections of the incoming photon and the target protons, and the notations $(\binom{\rightarrow}{\rightarrow})$ and $(\binom{\leftarrow}{\rightarrow})$ correspond to the initial states with the total spin equal to $\frac{3}{2}$ and $\frac{1}{2}$, respectively (see Fig. 4). Using the notation of Eq. (4) and

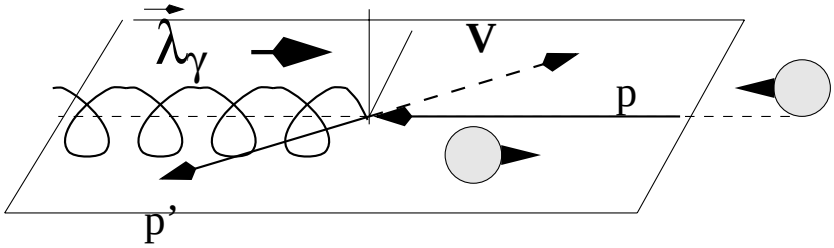

Figure 4: Beam-target asymmetry.

the expression for helicity-conserving amplitudes in Eq. (3), one can estimate C_{BT} in photoproduction at forward-angles as,

$$C^p_{BT} \simeq 2|\alpha^{pU}| \cos\delta^p_{\mathrm{N-U}}, \tag{5}$$

where α^{pU} is square root of the relative contribution of the unnatural parity exchange process in the total cross section

$$\alpha^{pU} \simeq \sqrt{\frac{\sigma^{pU}}{\sigma^p_{\mathrm{tot}}}} \tag{6}$$

and $\delta^p_{\mathrm{N-U}} \equiv \delta^p_{\mathrm{N}} - \delta^p_{\mathrm{U}}$, where δ^p_{N}, and δ^p_{U} are the phases of the natural and unnatural parity-exchange amplitudes, respectively. From this expression, one can understand that the beam-target asymmetry C_{BT} is very attractive as a tool for studying the contribution from exotic processes with unnatural-parity-exchange, because the asymmetry sensitively depends on α^U, but not on $|\alpha^U|^2$ [15].

The essential idea in physics here is that the beam-target asymmetry appears as an interference between the amplitudes with different parity-exchange properties. The phase

difference between diffractive photoproduction and pseudoscalar-exchange amplitudes is $\pi/2$ and the corresponding interference term disappears in C_{BT}. The phase difference between diffractive and knockout amplitudes is expected to be close to 0 or π, which leads to sizeable C_{BT} even at small $|\alpha^U|^2 \ll 1$.

However, it should be noted that there is another source to originate a finite beam-target asymmetry C_{BT} even at $\alpha^U = 0$. Actually, the Pomeron-exchange amplitude has a term responsible for the interaction of the proton and photon spins, which leads to the transition $\lambda_\gamma = \pm 1$, $m_i \to \lambda_\phi = 0$, m_f. The contribution of this amplitude decreases with increasing incident photon-energy, but remains to be important in a few GeV-region. It is clear that this term forbids the initial state with the total spin $\frac{3}{2}$ and leads to the finite and *negative* contribution to C_{BT}. This effect is expected to be small at forward angles.

Fig. 5(a) shows the beam-target asymmetry calculated without $s\bar{s}$ process as a function

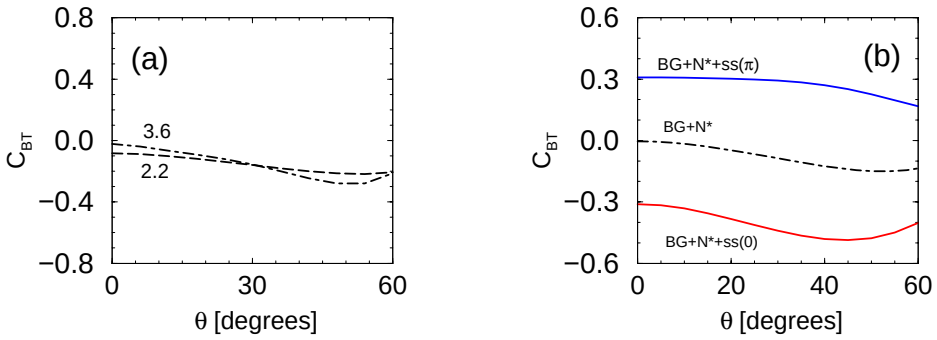

Figure 5: Beam-target asymmetry. (a) Beam-target asymmetry calculated without the $s\bar{s}$-knockout process at $E_\gamma = 2.2$ and 3.6 GeV. (b) Calculation without (dot-dashed curve) and with the knockout process at two different phases of $s\bar{s}$ configurations: π and 0, shown by upper and lower solid curves, respectively.

of ϕ-meson production angle in c.m.s. In this case the amplitude is dominated by the Pomeron-exchange and pseudoscalar-exchange processes. At large $|t|$, the resonant channel becomes important and it strongly modifies the beam-target asymmetry. However, its contribution is negligible at forward angles and C_{BT} is dominated by the Pomeron-exchange channel. The beam-target asymmetry, calculated by taking into account the $s\bar{s}$-knockout process at the relative phase $\delta_{N-U} = \pi(0)$ is shown in Fig. 5(b) by the upper (lower) curve. Since the background contribution from the Pomeron-exchange channel can be reliably estimated or canceled out, one can study the difference $|C_{BT} - C_{BT}^{BG}|$ or absolute value $|C_{BT}|$ which is not so sensitive to the unknown phase δ_{N-U}. Fig. 6 shows the absolute value $|C_{BT}|$, which is calculated by taking into account the $s\bar{s}$-knockout process as a function of initial photon energy at $|t| = 0.1$ GeV^2. For convenience, the beam-target asymmetry for background processes is also shown in Fig. 6. We also show the recent data point obtained from the work of the HERMES collaboration [16]. One can see that

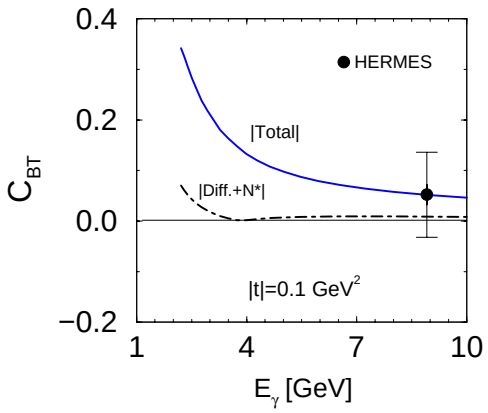

Figure 6: The absolute values of beam-target asymmetry calculated without the $s\bar{s}$-knockout (dot-dashed curve) and with the $s\bar{s}$-knockout process (solid line) as a function of E_γ at $|t| = 0.1$ GeV^2. The data point is taken from Ref. [16]

the contribution of the $s\bar{s}$-knockout process decreases monotonically with increasing E_γ, because of the corresponding dynamical factor ("form-factor") which decreases rapidly with increasing E_γ. One should note that the uncertainty for the choice of δ_{N-U} may amount to the order of 30% at $E_\gamma \leq 2.2$ GeV. This effect arises because of interplay of the knockout and N^* processes, suggesting that the measurement of the beam-target asymmetry in the energy region from 2 to 3 GeV is essential for extracting the $s\bar{s}$-content of nucleon.

To summarize this part we conclude:

1. The expected effect of the $s\bar{s}$ channel in the beam-target asymmetry in the $\gamma p \to \phi p$ process is large.

2. The optimum region for the study of this effect is $E_\gamma = 2 \sim 3$ GeV and $|t| \leq 0.4$ GeV^2.

2.1.3 Coherent photoproduction from deuteron

In the experiment with the circularly-polarized photon-beam and with the polarized-deuteron target, we have three initial spin states with the total spin projection J_z: $(\binom{\rightarrow}{\rightarrow}; J_z = 2)$ when the deuteron is polarized along the beam polarization, $(\binom{\leftarrow}{\rightarrow}; J_z = 0)$ when the deuteron is polarized along the opposite direction to the beam polarization, and $(\rightarrow\uparrow; J_z = 1)$ when the deuteron is polarized perpendicular to the beam polarization (see Fig. 7). Therefore, we have three beam-target asymmetries

$$C_{BT}^{21} = \frac{d\sigma(\binom{\rightarrow}{\rightarrow}) - d\sigma(\rightarrow\uparrow)}{d\sigma(\binom{\rightarrow}{\rightarrow}) + d\sigma(\rightarrow\uparrow)}$$

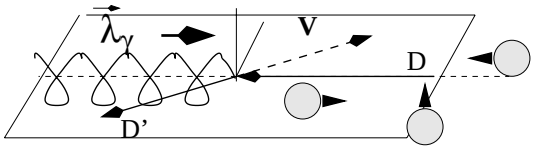

Figure 7: Beam-target asymmetry for the coherent photoproduction of ϕ-meson from deuteron.

$$
\begin{aligned}
C_{BT}^{20} &= \frac{d\sigma(\binom{\rightarrow}{\rightarrow}) - d\sigma(\binom{\leftarrow}{\rightarrow})}{d\sigma(\binom{\rightarrow}{\rightarrow}) + d\sigma(\binom{\leftarrow}{\rightarrow})} \\
C_{BT}^{10} &= \frac{d\sigma(\rightarrow\uparrow) - d\sigma(\binom{\leftarrow}{\rightarrow})}{d\sigma(\rightarrow\uparrow) + d\sigma(\binom{\leftarrow}{\rightarrow})}.
\end{aligned} \tag{7}
$$

Analysis of the coherent ϕ-meson photoproduction from deuteron performed in the work by Titov *et. al.* [18] gives the following conclusions:

1. The amplitude of photoproduction from deuteron, T^D, is proportional to the product of elementary isoscalar amplitude $T^s = (T^p + T^n)/2$ and the deuteron form factors $S^{N,U}$, which are different for the processes with natural and unnatural parity properties. As a result, the amplitude T^D decreases with $-t$ much faster than the elementary amplitude T^s, because the form factors $S^{N,U}$ decrease rapidly.

2. The elementary spin conserving amplitude T^s generates the spin conserving T^D-amplitude.

3. Unnatural parity-exchange transitions are suppressed for the deuteron target with spin projection $M_i = 0$.

4. The form factors of the natural parity-exchange (Pomeron) amplitudes with spin polarization $M_{i,f} = \pm 1$ and $M_{i,f} = 0$ are different : S_1^N decreases much faster with $|t|$ than the form factors S_0^N. Moreover, both of them are different from the unnatural parity-exchange form factor S_1^U.

5. Contribution of the isovector π-exchange amplitude is strongly suppressed.

6. $C_{BT}^{10} = -C_{BT}^{21}$.

Fig. 8 shows the differential cross section of the $\gamma D \to \phi D$ reaction as a function of $-t$ at $E_\gamma = 2.2$ GeV. One can see that the slope of $d\sigma^{\gamma D}/dt$ is steeper than that of $d\sigma^{\gamma p}/dt$, which has been shown in Fig. 3. However, the cross sections $d\sigma^{\gamma D}/dt$ at $|t| \sim |t_{\rm max}| \simeq 0.1 - 0.3$ GeV^2 will be measured with reasonable accuracy.

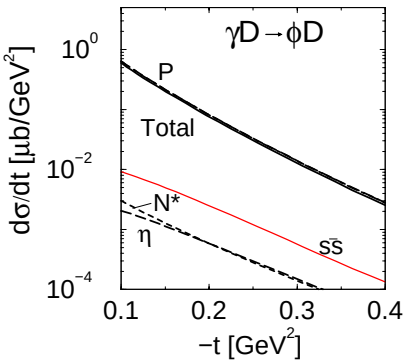

Figure 8: The differential cross section for the $\gamma D \to \phi D$-reaction as function of t at $E_\gamma = 2.2$ GeV.

Concerning to the beam-target asymmetries, it is found that the deuteron form factors lead to a difference in behavior and magnitude of the various beam-target asymmetries. The influence of the unnatural parity exotic component is strong and different in different asymmetries. The corresponding numerical calculations of C_{BT}^{21} and C_{BT}^{20} without and with the s$\bar{\text{s}}$-knockout process are shown in Fig. 9(a) by the dashed and solid curves, respectively. In the later case, we choose the phase $\delta_{N-U} = \pi$. Since the background contribution (the dashed lines in Fig. 9(a)) is under control, the difference $|C_{BT} - C_{BT}^{BG}|$ for different asymmetries will reflect the "phase-independent" effect of the s$\bar{\text{s}}$-knockout process. The corresponding prediction is shown in Fig. 9(b).

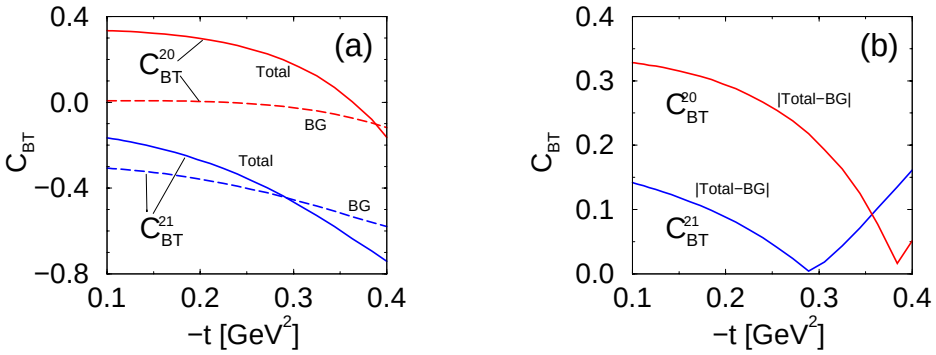

Figure 9: (a) Beam-target asymmetries C_{BT}^{21} and C_{BT}^{20} for the $\gamma D \to \phi D$ reaction without and with the s$\bar{\text{s}}$-knockout process shown by the dashed and solid curves, respectively. (b) The difference $|C_{BT} - C_{BT}^{BG}|$ for different asymmetries.

To summarize this part we conclude:

1. The cross section of coherent ϕ-meson photoproduction from deuteron at small $|t| \leq 0.3$ GeV^2 is comparable to the cross section for the $\gamma p \to \phi p$ reaction.

2. It would be interesting to measure, for the first time, the difference in the different beam-target asymmetries.

3. The analysis of the experimental data will show the manifestation of exotic processes ($s\bar{s}$-knockout), complementary to the $\gamma p \to \phi p$ reaction.

2.1.4 Incoherent photoproduction from deuteron

The total amplitude is a coherent sum of the photoproduction from the proton T^p and from the neutron T^n. But, if we do not identify recoil nucleons, the interference term between these two amplitudes from neutron and proton in a deuteron is proportional to the linear combination of the deuteron form factor, which depends on the spatial part of the momentum transfers $\mathbf{q}$, and becomes strongly suppressed relative to the direct terms (Note that the direct terms have not this suppression factor). Thus, the total cross section is proportional to the incoherent sum of cross sections of photoproduction from the individual nucleon on a deuteron, proton and neutron.

In the case of the experiment using a polarized target, we can measure three beam-target asymmetries (similar to the coherent photoproduction from deuteron): $\tilde{C}^{20}_{BT}$, $\tilde{C}^{21}_{BT}$ and $\tilde{C}^{10}_{BT} = -\tilde{C}^{21}_{BT}$. The close inspection of them leads to the following estimate

$$\begin{aligned} \tilde{C}^{20}_{BT} &\simeq \alpha^{pU} \cos\delta^{p}_{N-U} + \alpha^{nU} \cos\delta^{n}_{N-U}, \\ \tilde{C}^{21}_{BT} &\simeq \frac{1}{2}\tilde{C}^{20}_{BT}. \end{aligned} \tag{8}$$

Combining Eqs. (5) and (8), one can extract the effect of the $s\bar{s}$-knockout process from the neutron

$$\tilde{C}^{n}_{BT} \simeq 2\tilde{C}^{20}_{BT} - C^{p}_{BT}. \tag{9}$$

To summarize this part we conclude that the combined analysis of the photoproduction from proton and the incoherent photoproduction from the deuteron can give unique solutions to the exotic channels with unnatural parity exchange ($s\bar{s}$-knockout) in the photo-reaction with a neutron.

2.2 GDH sum rule

The Gerasimov-Drell-Hearn (GDH) sum rule relates to the total photo–absorption cross sections by a polarized nucleon with the anomalous magnetic moment. A simple relation between the integrated photo–absorption cross section value and the magnetic moment of a nucleon is deduced by assuming fundamental principles such as Lorenz invariance and gauge invariance, causality, and unitarity. This sum rule is now called as the GDH

sum rule, which was derived in the 1960's by Gerasimov [21] and by Drell and Hearn [22]. Hosoda and Yamamoto of Osaka University [23] derived the same formula independently in 1966 using a current algebra technique. The anomalous magnetic moment of the nucleon (κ^2) has a relation to the difference between the total cross sections with the nucleon spin parallel ($\sigma_{3/2}$) and anti-parallel ($\sigma_{1/2}$) to the circularly polarized photons, integrated as a function of photon energy (ν).

$$\int_0^\infty \frac{\sigma_{3/2} - \sigma_{1/2}}{\nu} d\nu = \frac{2\pi^2\alpha}{m^2}\kappa^2, \tag{10}$$

where m stands for nucleon mass. This sum rule for proton has been tested at ELSA (0.5 $\leq$ $E_\gamma \leq$ 3 GeV) and at Mainz (140 $\leq$ $E_\gamma \leq$ 800 MeV) [24, 25, 26]. Since the extensive measurements have been done in these five years, there seems nothing to be left for the GDH sum rule on proton. The remaining problems on proton are to measure the GDH sum rule at low energy and at very high energies.

The GDH sum rule measurement on neutron is the next subject to be done. If experimental results on proton and neutron are consistent with the respective GDH_p and GDH_n predictions, taking into account the large uncertainties of the partial wave parameterization, the proton-neutron difference comes out four times too large and with the opposite sign compared to GDH_{p-n} predictions [27]. Recent experimental results on GDH_p up to 800 MeV photon energy [25] show that saturation of the sum is already significantly achieved and the GDH sum rule is roughly verified for the proton. As the results, the large deviation from GDH_{p-n}, must be attributed to the neutron [28] which should be measured in an independent GDH experiment.

For this purpose, we definitely need to measure the GDH sum-rule values with the polarized deuterium target for extracting GDH_n. The HD target presently proposed is ideal for this experiment. In the case of the deuteron experiment, the problem associated with the extraction of neutron information is serious for our thinking. If the coherent effect in photoproduction happens in extracting the neutron GDH sum rule from the deuteron target consisting of proton and neutron, we cannot get the true information on the GDH sum rule on neutron. In order to check all the possibilities of coherent effects, we need the precise measurements of all the photoproduction channels together with the theoretical examinations.

It should be noted here that the trial of measuring the GDH sum-rule value for neutron has been already started at Mainz, Bonn, and GRAAL. At SPring-8, much precise measurements of the high energy contribution of the GDH sum rule will be possible with the HD target thanks to a high energy and high polarized photon beam. A similar experiment at SPring-8 proposed by Iwata *et al.* [31] has also been approved by RCNP-QPAC.

The total photo-absorption cross sections in the energy range of 1.5$\sim$3.0 GeV will provide a means of checking the QCD model [29, 30]. Measurements of the GDH sum

rule at four facilities in different energy regions will be complementary to each other because the test of the sum rule and the QCD model requires the cross section data in the wide energy region.

The Compton scattering experiment from proton is complementary to the GDH experiment. Gell-Mann, Goldberger, and Thirring describe the Compton scattering between the polarized photon and polarized proton [32] and point out that the Compton scattering relates to the proton magnetic moment and the charge distribution of proton. Thus, if we can measure the extremely small cross sections for Compton scattering at 1.5$\sim$3.0 GeV, the experiment will provide detailed information on the microscopic structure of proton and neutron.

2.3 Other reactions

At SPring-8, the interference effect between the Pomeron exchange and knock-out process will be most suitably studied with a circularly polarized photon-beam and a polarized proton target. Similar measurements are feasible for the ω and η meson photoproduction. There are already a plenty of papers published in the market associated with these subjects [19, 20]. Since the low momentum-transfer data ($-t\leq$ 1 GeV^2) can be interpreted in the framework of the vector-meson dominance (VMD) model, the beam target asymmetry for ω and η meson photoproductions gives us useful information on the associated exchanged particles (Pomeron, π-meson, and gluons) through the theoretical calculations on the basis of the QCD-inspired models.

Double polarization measurements in K photoproduction will have strong impacts to effective theories with baryon resonances [33]. The baryon spectrum described in the framework of ud quarks has been identified by $\pi + N$ and the (γ,π) reactions. However, there are still many "missing resonance" states, which are predicted in the quark models and are not observed experimentally. A predicting power of the baryon spectrum is now a touchstone to examine the validity of the effective theories. The experimental studies of the photoproduction reaction associated with strange quarks are expected to open new eyes to look at the baryon spectrum. For example, the experimental studies of the kaon photoproduction reaction had a considerable progress in recent years, because of the new operations of the photoreaction experiments. The proposed new experiment will give significant contributions to develop hadron physics.

3 Polarized HD target

Heteronuclear Hydrogen molecules like HD can be polarized and have interesting properties. The proton with spin 1/2 and the deuteron with spin 1 are independently polarized

and are independently reversible. In HD, H and D vector polarizations, exceeding 95% and 70%, respectively, are attainable with the present low-temperature and high-magnetic-field technology. Solid polarized HD samples are kept in the frozen-spin conditions for temperatures below 4 K at moderate holding fields (0.5 T), allowing easy transportation. Therefore, the polarization production site can be separated from the experimental one [34]. For nuclear physics experiments, thick targets of several moles (20 cm^3/mole) can be produced, making it possible to use them with low-intensity real-photon beams [35]. We can expect relaxation times larger than a week for H and longer than a month for D at 0.5 K and 0.5 T [36], which is enough to perform experiments using a rather simple In-Beam Cryostat (IBC) [37].

In order to achieve high polarizations of proton and deuteron targets, we employ the static method using "brute force" to polarize the protons in HD at low temperature (15 mK) and high field (17 T), and the adiabatic fast passage technique is applied to transfer this polarization to the deuterons. Due to long relaxation times, a full production cycle is longer than a month.

3.1 Polarization mechanism of the HD target

The history of the frozen-spin molecular HD target proposed firstly in 1967 [38] is very long and can date back retroactively to 1957. Honing first suggested that the proton polarization in a solid HD target can be explained on the basis of the experimental observation of relaxation times influenced with ortho-hydrogen impurities [39]. In Table 1, we list the mile stone events for the remarkable developments associated with the HD target. With longstanding great efforts by the Syracuse, BNL and ORSAY groups, this HD system is now being used for the actual experiments at LEGS and GRAAL. Although there are still many technical problems to improve the performance of the HD system, the principal developments seem to finish for preparing the HD system.

We will here outline the principle of polarized HD target in an intuitive way. Fig. 10 shows a schematic view of the process of the polarized HD target. The basic symmetry condition imposed on the total wave functions of H_2 (two fermions) and D_2 (two bosons) gives a restriction on the possible nuclear spin orientation at low temperature. For H_2, the so called ortho state has nuclear spin S=1 and molecular orbital angular momentum L=odd. Since the nuclear spins are aligned, o-H_2 can be polarized. However, the equilibrium condition at low temperatures requires the para-hydrogen state with S=0 and L=0. Here, since the nuclear magnetic moments are anti-parallel, the sample cannot be polarized. In the case of Deuterium, it is the p-D_2 combination (S=1; L=odd) that disappears at low temperature, leaving the o-D_2 (S=0,2; L=0). Although 5/6 of the nuclei in this state have their spins parallel (S=2), the small magnetic moment of the deuteron makes

Table 1: History of polarized HD targets.

1957	M. Bloom	An important relaxation mechanism for the protons in solid HD: via "impurity" ortho-H_2 molecules.
1966	W.N. Hardy and J.R. Gaines	The above relaxation mechanism with o-H_2 was confirmed by relaxation time measurements in very pure HD at 1.2 K $\sim$ 4.2 K $\rightarrow$ proton relaxation time of many hours was obtained by aging a solid HD with a small o-H_2 impurity.
1967	A. Honig	Proposal for a frozen-spin target: polarizing the HD at · high magnetic field ($>$ 10 T) · low temperature (near 10 mK)
1968–1978		Study of the relaxation times, depending on temperature, magnetic field, ortho-H_2 and para-D_2 concentration.
(1968–1978)	A. Honig, *et al.*	At Syracuse University · $T = 0.4 \sim 16$ K, $B = 0 \sim 1$ T
(1971–1977)	H.M. Bozler, E.H. Graf, *et al.*	At SUNY Stony Brook · $T = 35$ mK ~ 4 K, $B = 1.5 \sim 10$ T
1975	H. Mano and A. Honig	Radiation damage was studied at BNL 28 GeV proton synchrotron and Cornell 10.4 GeV electron synchrotron.
1976	A. Honig and H. Mano	RF forbidden transition adiabatic rapid passage Proton $\Leftrightarrow$ deuteron polarization transfer.
1983–late 1980s	A. Honig, *et al.*	The first application of polarized HD (produced at Syracuse for fusion study).
1991	N. Alexander, *et al.*	Invention of cold-transport devices for moving HD from production site to experimental site.
2001.11	LEGS collaboration	The first double-polarization data of meson photoproduction with polarized HD target

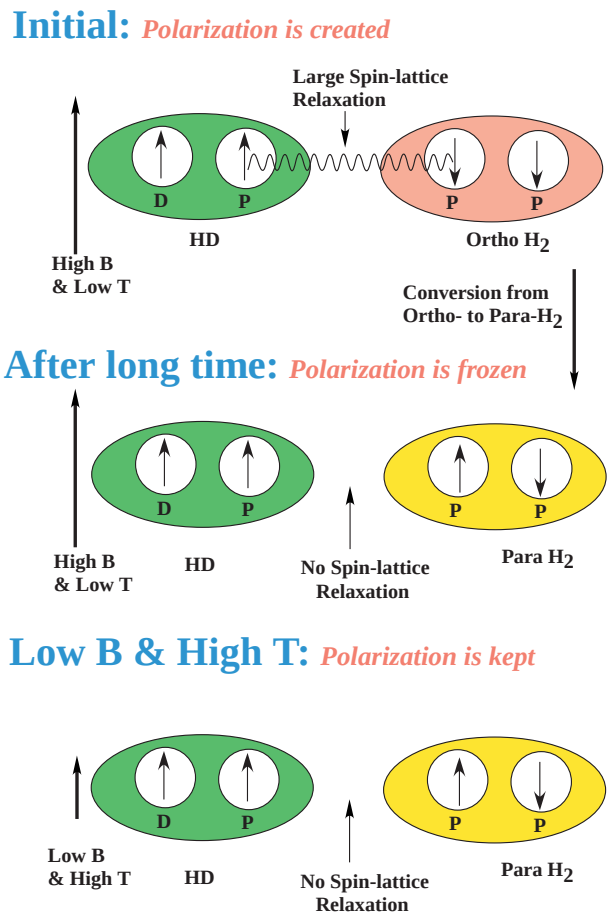

Figure 10: An intuitive picture showing a principle of HD target

static polarization of pure Deuterium very difficult.

In contrast, the orbital and spin angular momenta of the heteronuclear molecules HD are not limited by symmetry requirements (one fermion and one boson) and hence can be in the molecular rotation state L=0 independent of the relative orientation by spin 1/2 and spin 1 species at low temperature. Since the spin-lattice coupling is primarily caused in the process of molecular rotations, the relaxation rates are extraordinary small. Although this long relaxation time is essential for the usage of polarized targets in nuclear physics experiments, it makes the polarization phase equally long. This is a dilemma; we hope to prepare the polarized target in a relatively short time and like to keep the produced polarized target for a long time in experiments. For the polarization of HD, the solution to this dilemma was suggested by Honig in 1967 [38].

The relaxation (polarization) time can be reduced by introducing small (approximately the order of 10^{-4}) contamination of o-H_2 and p-D_2, as an impurity. The presence of o-H_2 and p-D_2 plays an important role to polarize the target. The molecular orbital angular momentum couples with both the lattice and the nuclear spin. Thus, by doping small

amounts of o-H_2 and p-D_2 into the pure HD, the relaxation times of the H and D in HD are reduced so that the sample can be polarized. The equilibrium polarizations of 80% for H and 20% (vector) for D can be achieved in this way for HD cooled to 15∼20 mK in a Dilution Refrigerator at the magnetic field of 17 T. The polarization of H can be reached at 95% at mK. The sample must be kept at the temperature of 15∼20 mK and under the field conditions long enough to let the impurities o-H_2 and p-D_2 decay to their magnetically-inert ground states, so that the sample spins are effectively "frozen". In view of the corresponding decay time constants, this aging process can be very long (40 days to reach H relaxation times longer than a week at 4 K and 0.5 T) and become prohibitive for D. Furthermore, the D polarization is only 20%. Therefore, in the practical cycle which has been used to polarize HD, only o-H_2 doping has been used to polarize H. The D polarization has been obtained by transferring the H polarization to the D, using a method commonly known as "Adiabatic Fast Passage" [40]. This technique takes advantage of the dipole coupling of H and D nuclei in different HD molecules. In this way, the polarization of deuteron reaches at 70% [34, 36].

3.2 HD target development at ORSAY

Figure 11 shows a schematic view of the existing HYDILE (HYdrogen Deuterium for Intersecting Laser Electron beams) target developed at the Institut de Physique Nucleaire (IPN), ORSAY. It is presently under construction within a French-Italian (IN2P3-INFN) collaboration, to perform photoproduction experiments using the fully polarized high-energy backscattered-photon beams with the GRAAL set-up at the European Synchrotron Facility (ESRF) in Grenoble (France).

The only impurities in the HD material are thin Al wires which are necessary to insure the cooling. They represent at most 20% in weight of the HD content. For 5 cm of HD, the target thickness is 720 mg/cm^2, while the total thickness of Kel-F windows is of the order of 150 mg/cm^2. The IBC provides the cooling of the HD sample at a temperature of 0.5 K and the polarization holding field, through a 1 mm thick superconducting coil (NbTi) attached to the 4K ^{4}He shielding cryostat. The maximum field is 1 Tesla, allowing relaxation times of more than one week, for both H and D. Saddle coils are foreseen, with a transverse 1 Tesla field, allowing to rotate the spin in the transverse orientation, or to reverse the polarization directions.

Equipment for producing polarized HD targets is now operating at IPN-Orsay (France). The main piece to give a high polarization of HD is a powerful ^{3}He$-^4$He Dilution Refrigerator (DR) fabricated by Leiden Cryogenics BV, with a heat lift capacity of 12 μW at 10 mK. A circulation rate of 5 mmole/s of ^{3}He can be sustained, resulting in a cooling power of 3.8 mW at 110 mK. The base temperature measured on the mixing chamber is below 4

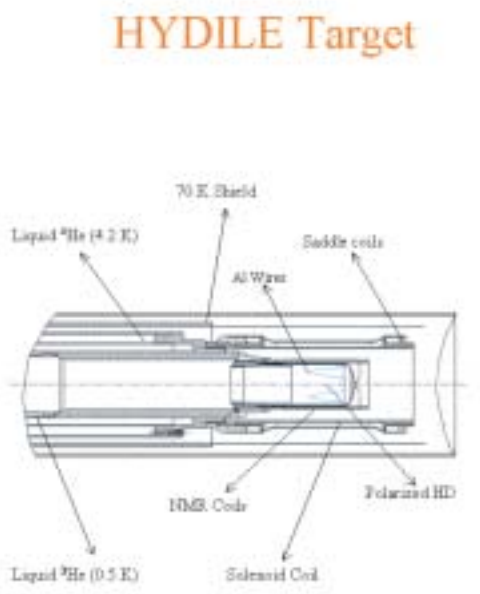

Figure 11: View of the HYDILE polarized HD target inside the In-Beam Cryostat (IBC) constructed at IPN-Orsay.

mK. The refrigerator is equipped with a 13.5 T superconducting NbSn coil having a bore diameter of 72 mm, a bore length of 53 cm and a field homogeneity of 4.3×10^{-4}.

Solid HD samples are made with a dedicated cryostat, called "Ice Maker" (IM), before the polarization process. This is a ^{4}He cryostat equipped with a 100K-1.5K variable temperature insert and a 2.5 T superconducting coil. This cryostat is also used for the storage and transport of HD polarized targets. In this sense, the IM is also called as Storage Cryostat (SC). In order to handle the targets between the DR and the IM, a 4.2K telescopic Transfer Cryostat (TC) has been constructed at Orsay. Basically, a left-hand right-hand thread mechanism makes it possible to engage, screw or unscrew a target in or from its cold finger, while an 0.5 T superconducting coil provides a magnetic field sufficient to hold the target polarization during the period of the "cold transfer" process of HD from the DR to the IBC.

3.3 Achievement of the HD target

The first attempt to polarize a 1 mole HD target has been done at Orsay in October 1999 with the main goal of putting the DR together with its NMR measurement probe into a first full operation cycle. The results of this first test are reported in Ref. [41]. A second polarization run was performed in July 2000, in order to establish the polarization rates and the relaxation times attainable with the present system together with the accuracy of absolute polarization measurements. The corresponding results are given in Ref. [42]. More recently, another polarization was attempted, in order to demonstrate the ability of the system to transfer polarized samples from the DR to the IM. The HD targets were made from commercially available HD gas with high initial H_2 and D_2 impurities of 1.1% and 0.5%, respectively. Small impurities of ortho (o-H_2) and para (p-D_2) are necessary for the polarization process. However, the above values are at least 10 times bigger than the ideal value of impurity [38]. Under such unfavored conditions, the relaxation times are expected to be short. Nevertheless, we could successfully transfer a polarized sample with a loss of polarization of 35%. The polarization rates for protons and deuterons were, respectively, 60% and 14% before the transfer. With double distilled HD, as available in US from recently working distillation [43], relaxation times as long as 5 days have been achieved. We found that the polarization loss during the transfer was negligible. The last polarization run performed at Orsay in spring 2002, using double distilled HD from the LEGS Spin Collaboration, has reproduced the results that have been already obtained at BNL. Figure 12 shows how the relaxation time T_1^H evolves with aging, as a function of the temperature and holding fields. A simulation of a transfer, maintaining the target for more than one hour at the field and temperature of the TC, resulted in a polarization loss less than 3%.

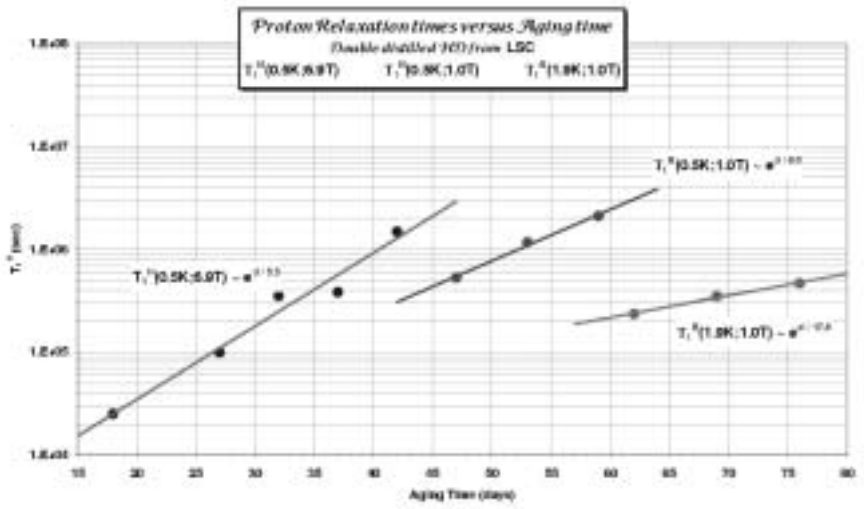

Figure 12: Evolution of the relaxation time T_1^H, as a function of aging, at different values of the temperature and holding field.

Now, after these efforts at BNL and ORSAY over many years, it has been found that the H polarization reaches at 90% and the D vector polarization exceeds 50%. The H and D can be polarized independently and their relative orientation can be either parallel or anti-parallel [38]. Relaxation times for H and D reach at one week and one month, respectively.

In the configuration depicted in Figure 11, the saddle coils are clamped with the solenoidal coil. It becomes possible, using appropriate variations of the current intensities in the coils, to rotate adiabatically the spins and put them in a transverse direction. It has been shown that the saddle coils alone can produce, in the target volume, a transverse field with an homogeneity better than 2.5% and a polar angle with the transverse axis less than 2.5°, in spite of the constraints imposed by the geometry of the system. This is particularly true if only the limited interaction region between the collimated backscattered beam and the target is considered [44].

3.4 The GRAAL experiment with the polarized HD target

3.4.1 The GDH Sum Rules

The GRAAL program with the polarized HD target HYDILE will be the test of the Gerasimov Drell-Hearn sum rule (GDH) for both proton (GDH_p) and neutron (GDH_n)

[21, 22]. A first experimental investigation of GDH_p up to the 800 MeV photon energy [24, 45], followed by a recent experiment up to 3 GeV [46], where saturation of the sum is significantly achieved, shows that the GDH sum rule is reasonably verified for the proton. Indeed, recent parameterization in the framework of dynamical models predicts a correct value for GDH_p but miss GDH_n [28] significantly . However, a recent electron scattering experiment on a polarized ^{3}He gas target (considered as a polarized neutron target), conducted to very small Q^2 (0.1 GeV^2) [47] and extrapolated to the real photon point [48], seems to be consistent with the GDH_n prediction. Anyway, the GDH predictions are valid for real photons only; therefore it is of prime importance to verify experimentally the GDH predictions for GDH_p, GDH_n and GDH_{p-n}. Polarized HD, containing at the same time polarized protons and deuterons with high effective polarizations, used as a target on the fully polarized backscattered real photon beams available at LEGS, GRAAL or SPring-8, would be ideally suited to this aim. A direct comparison between photoproduction cross sections (σ), taking place on equally polarized loosely bound proton and neutron from the polarized D nucleus and the free proton (Fp) from the polarized H nucleus, is required to verify GDH_n. At GRAAL, the sensitive second and third resonance region (500 MeV$\leq E_\gamma \leq$1.5 GeV) can be scanned.

3.4.2 Experimental Considerations

Present unpolarized GRAAL data [49] show that the GRAAL experimental conditions are very favorable to verify both GDH_p and GDH_n. The GRAAL trigger, requiring a significant energy loss in the BGO ball, is almost insensitive to the electromagnetic background which is mainly forward peaked and has therefore little chance to deposit a sizable energy into the BGO. The acceptance of the entire detector LAGRANγE being larger than 95% of 4π, the efficiency of the above described GRAAL trigger is always above 90% for any final state. Therefore, the counting rates can be directly related to the total cross section σ_T. In addition, the contribution of the empty target is less than 20% in the raw data and almost negligible after data analysis. As a consequence of the above experimental facts, σ_T has been deduced by a simple "Subtraction" method: [Target full - Target empty] for both the unpolarized liquid H_2 and D_2 targets used up to now. Figure 13 shows those data for an H_2 target.

It has also been demonstrated that, although the GRAAL set-up is ideally suited for neutral channels because of the BGO ball [50], charged channels can be isolated by using appropriate algorithms [51]. Figure 13 shows that σ_T can also be obtained by summing individual channels. This method is called the "Summing" method. Deviations between the two methods appear in the energy region higher than 1.2 GeV, because the contributions from K mesons and Vector mesons have not yet been taken into account.

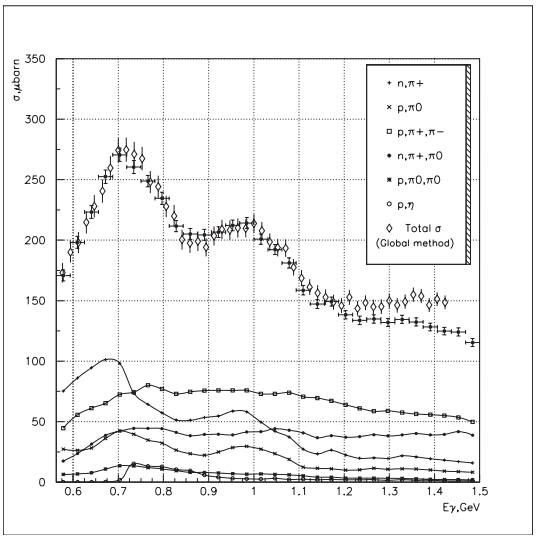

Figure 13: Total photoproduction cross sections on the proton. The open diamonds: "Subtraction" (global) method. Full points: "Summing" of partial channels.

At the present stage, the experimental challenge is to measure how much σ_d, the cross section on the deuteron, differs from the sum of σ_p and σ_n; σ_n being the cross section which would be measured on an unaccessible free neutron (Fn) target. One possible procedure is to use Quasi Free (QF) reactions, taking place on the loosely bound "p" and "n" in the polarized D, for the channels with neutral pions, which are easily identified by the GRAAL set-up. It has been shown in Ref. [52] that π^0 data can be measured with an unprecedented accuracy on the free proton (Fp) target. It has also been shown by data taken by some of us at Bonn [53] and preliminary data from GRAAL on a D_2 target that the Quisi-free (QF) peaks can be well identified in η meson photoproductions on "p" and "n". The method is to detect in coincidence the π^0 or η in the BGO ball and the recoil from the QFp or QFn in the forward walls. In the GRAAL technique, the detection method is the same for both "p" and "n" (based essentially on TOF); therefore, kinematical cuts can be identical for QFp and QFn reactions. The ratio $\sigma_{QFn}/\sigma_{QFp}$ is precisely measured in this procedure by a simple ratio of counting rates. The only parameter is the neutron detection efficiency, but for the neutron energies considered here, neutron detection efficiencies can be rather precisely estimated. One can assume that in QF reactions, the ratio $\sigma_{QFn}/\sigma_{QFp}$ is very close to the ratio σ_{Fn}/σ_{Fp} for free nucleons, because rescattering contributions are small (of the order of a few % as estimated by L'vov [54]). Finally, the good knowledge of the ratio σ_{Fn}/σ_{Fp} for several dominant channels, measured on polarized D together with the genuine σ_{Fp} from the polarized H, provides values entering in simple mathematical formulas allowing to derive fairly precisely σ_{Fn} for helicity states 1/2 and 3/2, namely the quantities necessary to verify $\mathrm{GDH_n}$ experimentally.

A similar procedure in the GDH sum-rule measurement can be applicable with very careful checks of the detailed performance of the LEPS spectrometer.

3.4.3 Schedule

The essential instruments that are needed to implant HYDILE on the GRAAL beam line are the IBC, the GRAAL TC, and a transport support for the SC. All these devices are under final testing at Orsay and will be moved to Grenoble in May 2003. The aim is to perform a commissioning experiment on polarized protons in June-July 2003 and real data taking experiments starting from September 2003 and so on. Figure 14 shows

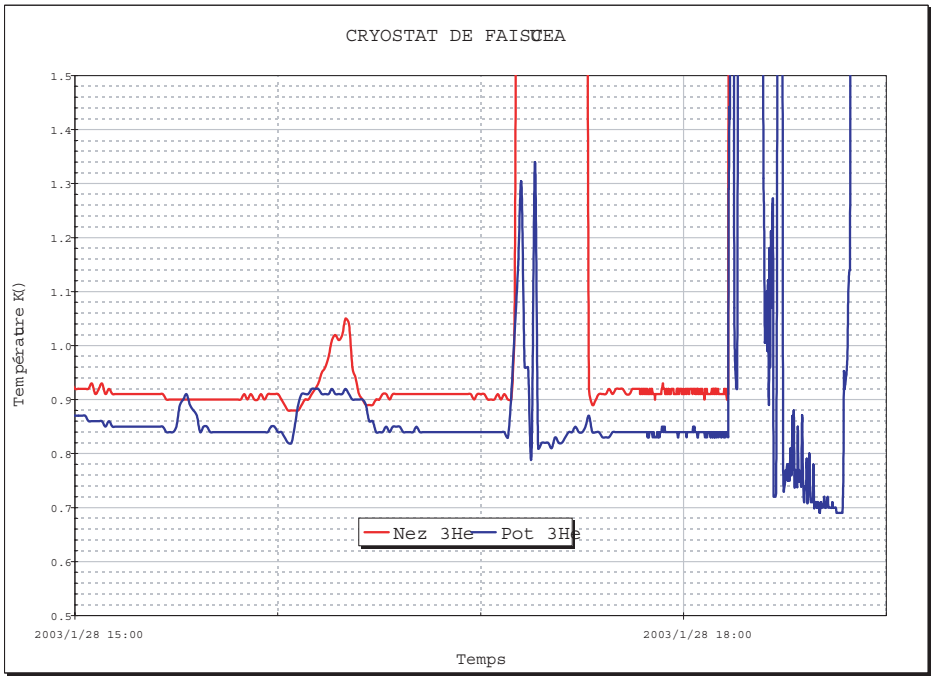

Figure 14: A record of the temperature reached by the GRAAL IBC.

a record of the temperature reached by the GRAAL IBC, which allows to anticipate a running temperature of the polarized HD sample around 1 K. Given a holding field of 1.4 Tesla, we can anticipate an on-beam relaxation time of 6 days, after 60 days of aging (see Fig. 12 concerning the relaxation times).

4 Status of the SPring-8 experiments

4.1 Laser electron photon beam at SPring-8

Polarized photon beams are produced by the backward Compton scattering process from the head-on collision between the polarized laser lights and the 8 GeV electrons. A typical

power of the argon laser, which is usually used in the LEPS experiment, is 5 W in the case of multi-UV mode (∼350 nm). The laser gives a tagged photon beam ($1.5 < E_\gamma <$ 2.4 GeV) with an intensity of about 10^6/s. We have carried out experiments with a linearly polarized photon beam for a few years after the construction of the SPring-8 experimental facility. A typical linear polarization degree of the injected laser is close to 100%, which produces a photon beam with a polarization degree higher than 90% at the maximum photon beam energy of 2.4 GeV.

Although the technique for obtaining the circularly polarized photon beam have not been completely established yet, the development itself has arrived at the final stage. Generally, the polarization degree of the circularly polarized laser is measured after transferring to linearly polarized laser by using a $\lambda/4$ plate. Figure 15 shows the output of a photodiode when a polarizer in front of the photodiode is rotated. The flat distribution

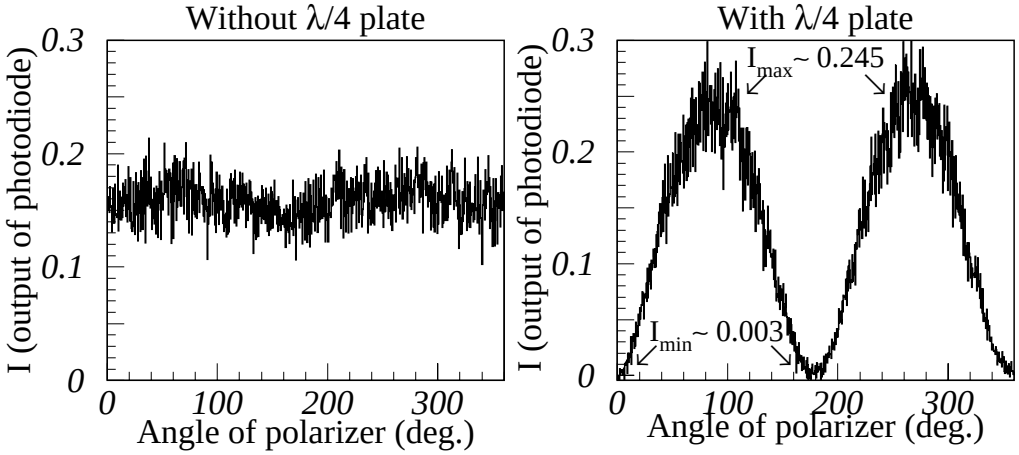

Figure 15: Output of the photodiode when the polarizer is rotated. The left and right panels show the results of the photodiode measurements without and with the $\lambda/4$ plate, respectively.

shown in the left panel of Fig. 15 indicates that the laser is unpolarized or circularly polarized. The right panel of Fig.15 shows that the laser with a $\lambda/4$ plate is transferred to linearly polarized laser. Combining two results shown in Fig. 15, we can conclude that the original laser is circularly polarized. Since the polarization degree (P_{laser}) is defined as,

$$P_{laser} = \frac{I_{max} - I_{min}}{I_{max} + I_{min}}, \tag{11}$$

we get $P_{laser} \sim 98$ % for a circularly polarized laser. This polarization degree is good enough to produce highly circular-polarized photons.

The laser with a wavelength of 266 nm which produces photon beams with energies of 1.5∼2.9 GeV is under development. We tested the linearly polarized laser with a power of 1.3 W once and it gave a tagged beam intensity of about 2×10^5/s. The polarization degree will be checked in near future.

4.2 Overview of the LEPS spectrometer

In the experimental hutch, we have built the LEPS detector which is optimized for the measurement of charged mesons at forward angles. The detector consists of a plastic scintillator after a target (STC), an aerogel Cherenkov counter (AC), silicon-microstrip detector (SVTX), three drift chambers (DC1, DC2, and DC3), a dipole magnet, and time-of-flight (TOF) counters (Fig. 16).

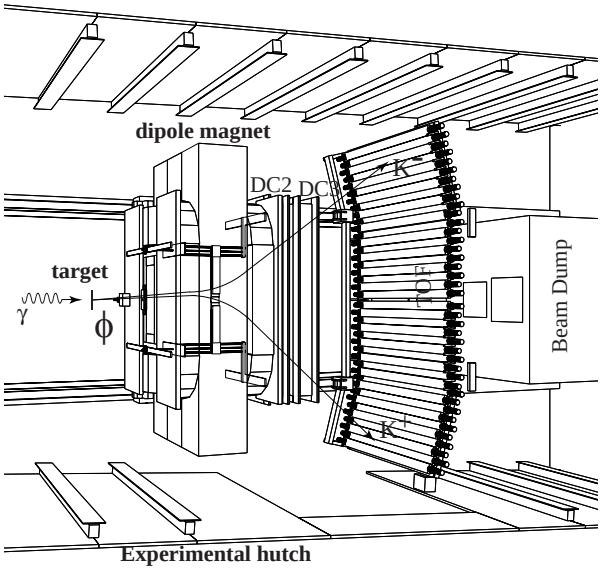

Figure 16: Top view of the LEPS detector in the experimental hutch. The photon beam is injected to the target from the left side. A typical event of K^+K^- pairs decaying from ϕ meson is illustrated. Charged particles are bent by the 30 ton dipole magnet and their trajectories are determined by the multiwire drift chambers (DC's) triggered with the TOF counters.

The opening of the dipole magnet is 135-cm wide × 55-cm high, and the length of the pole is 60 cm. The field strength at the center is 0.7 T. The trigger requires a tagging counter hit, charged particles after the target, and at least one hit on the TOF counters. Electrons, positrons, and high energy pions are vetoed by requiring no signal from the Cherenkov counter. In order to measure the momentum of the charged particles, their trajectories are measured with the two planes of single-sided silicon-microstrip detectors and the six-plane multiwire drift chamber (MWDC) placed upstream of the dipole magnet,

and two sets of five-plane MWDC's after the dipole magnet. In order to collect the data from different detectors and readout circuits via a fast computer network, a new data acquisition system has been developed [55, 56]. The angle coverage of the spectrometer is about ± 0.4 rad and ± 0.2 rad in the horizontal and vertical directions, respectively. The momentum resolution for 1-GeV/c particles is about 6 MeV/c.

The particle identification is performed by measuring the time of flight (TOF) of momentum-analyzed particles from the target to the TOF wall. The spectra of the reconstructed mass is shown in Fig. 17. The mass resolution is about 30 MeV/c^2 for 1-GeV/c

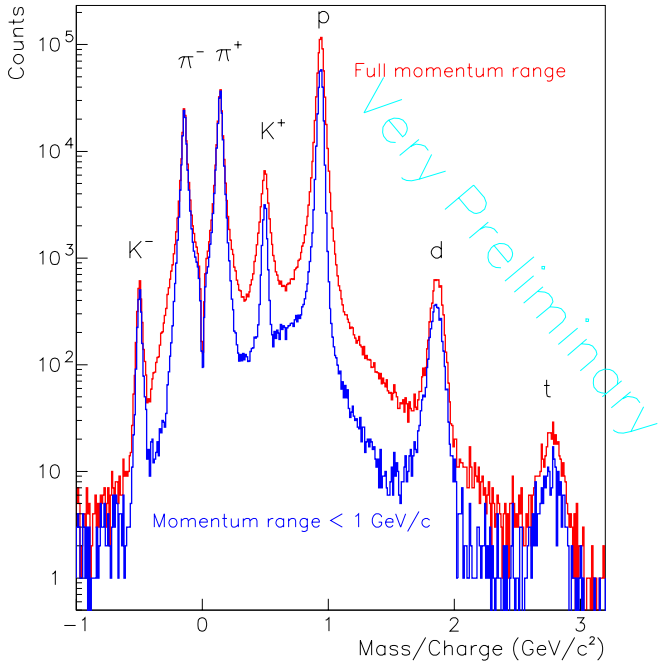

Figure 17: Reconstructed mass spectra. Blue and red histograms are mass of particles with the momentum smaller than 1 GeV/c and in the full momentum range, respectively.

kaon. The first physics run with a liquid hydrogen target started in December 2000.

4.3 Detector development

4.3.1 Time projection chamber

A time projection chamber (TPC) has been built for the measurement of hadron photoproduction with 4π acceptance. The primary purpose of the TPC is to study the nature of $\Lambda(1405)$ via the photoproduction in nuclei [57]. The decay particles Σ (decaying into π and N) and π are detected with the TPC. The invariant mass spectra for $\Sigma\pi$ will be a

good probe to study the properties of $\Lambda(1405)$. The TPC will be is also used as a general-purpose detector for various reactions. The detector itself has been already completed as shown in Fig. 18 and 19, although the fine tuning of the system is now underway.

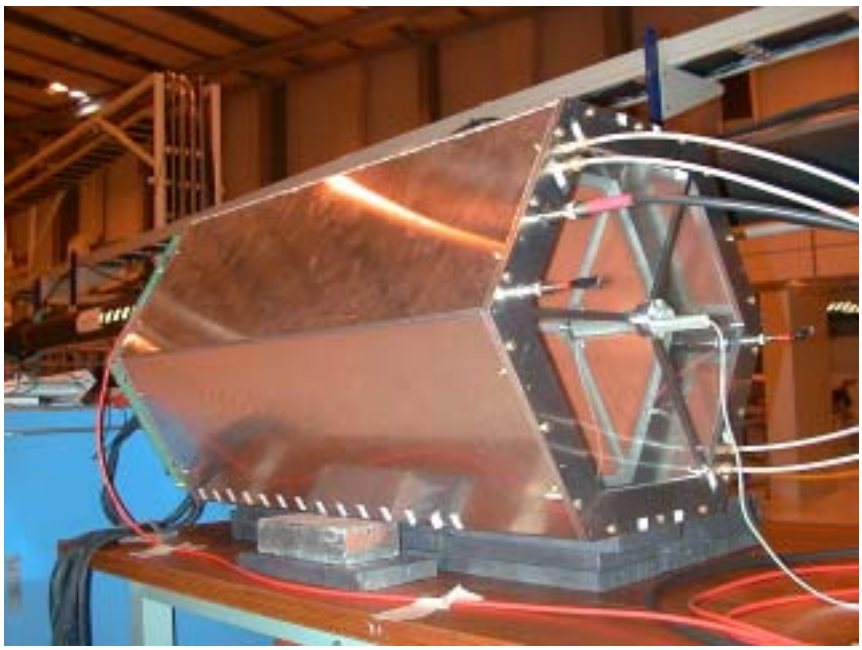

Figure 18: A picture of the time projection chamber.

The test of readout circuit and the detector performance will be finished soon. The first experiment with the TPC will be performed in 2003. The size of the TPC is 700 mm in length and 350 mm in radius with a cylindrical-shape active volume. From the test using cosmic muons, the spatial resolution 280 μm and 620 μm has been obtained in the pad (xy) plane and along the drift (z) direction, respectively [58].

4.3.2 GDH sum rule experiment

A proposal of the GDH sum rule measurement was approved at QPAC (PAC for the LEPS public-use beamtime) in 2001 [59]. In the proposal, a polarized target using dynamical nuclear polarization (DNP) method is planned to be used. Polyethylene will be used as target material. They plan to install a dilution refrigerator that was used for the KEK polarized target [60]. The refrigerator has a cooling power of about several mW at 0.3 K. They also propose to use the existing superconducting solenoid magnet to produce 2.5 T magnetic field with 10^{-4} homogeneity for 50-mm long $\times$ 30 mm$^{\phi}$ volume around the target. They propose to perform the measurement without using the LEPS spectrometer or TPC and planning to construct a new detector system optimized for the total cross section measurement. Both the polarized target and the detector system have not been constructed yet.

Figure 19: The TPC and the superconducting solenoid.

5 Recent results from LEPS with unpolarized targets

5.1 ϕ photo-production near threshold

Since a ϕ meson is almost pure $s\bar{s}$ state, diffractive photo-production of a ϕ meson off a proton in a wide energy range is well described as a pomeron-exchange (multi gluon-exchange) process in the framework of the Regge theory and of the Vector Dominance Model (VDM) [61]; a high energy photon converts into a ϕ meson and then it is scattered from a proton by an exchange of the pomeron [62, 63, 64] while the meson-exchange is suppressed by the OZI rule. However, other contributions arising from the meson (π, η)-exchange [64], scaler (0^{++} glueball)-exchange [65], and $s\bar{s}$ knock-out [66] processes get increased at low energies. These contributions fall off rapidly when the incident γ-ray energy increases, and can be studied only in the low energy region near the production threshold. Linearly polarized photons are an ideal probe to decompose these contributions. For natural-parity exchange such as pomeron and 0^{++} glueball exchanges, the decay plane of K^+K^- is concentrated in the direction of the photon polarization vector. For unnatural-parity exchange processes like π and η exchange processes, it is perpendicular to the polarization vector.

The invariant mass distribution of identified K^+K^- pairs is shown in Fig. 20. The fitted peak position of 1019.4 ± 0.1 MeV is consistent with the world data average. Fig. 21 shows the measured azimuthal decay-angle distribution of the K^+ relative to the photon

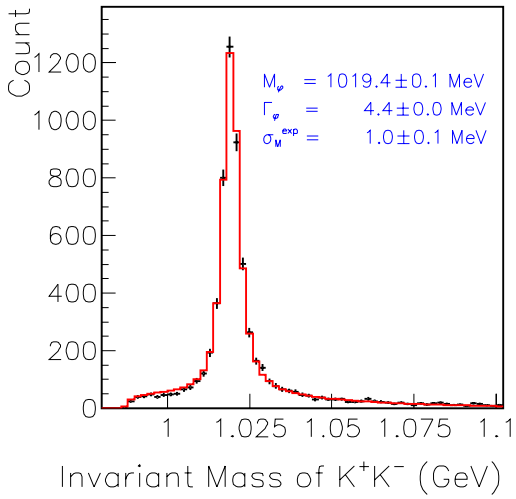

Figure 20: The invariant mass distribution of identified K^+K^- pairs.

polarization in the helicity system for $2.2 < E_\gamma < 2.4$ GeV and $-0.2 < t < 0.0$ $(\mathrm{GeV}/c)^2$. No acceptance correction is applied. However, in the present case, the correction is expected to be small for the chosen E_γ and t region. It is clear that the contribution from the natural-parity exchange process is a large fraction in the total scattering amplitude at the energy as low as $E_\gamma = 2.3$ GeV since the angular distribution peaks at 0° and 180°.

5.2 K^+ photo-production

Recent measurements for $K^+\Lambda$ photo-production at SAPHIR indicated a structure around $W = 1.9$ GeV in the total cross-section [67]. It attracted theorist's interest to study missing nucleon resonances in this process. Mart and Bennhold [68] showed that the SAPHIR data can be reproduced by inclusion of a new D_{13} resonance which have large couplings both to the photo- and $K\Lambda$-channels according to the quark model calculation [69]. Although it is difficult to draw a strong conclusion on the existence of D_{13} resonance from the cross-section measurements, the photon polarization asymmetry is very sensitive to the missing nucleon resonance. The LEPS collaboration has measured the asymmetry observables in the photon-beam energy region of 1.5∼2.4 GeV [74], while the measurement below 1.5 GeV has been carried out at GRAAL [70]. Fig. 22 shows a missing mass spectrum for the (γ,K$^+$) reactions. About 73,000 events and 49,000 events were collected for $K^+\Lambda(1116)$ and $K^+\Sigma^0(1192)$ productions, respectively. Fig. 23 shows the photon

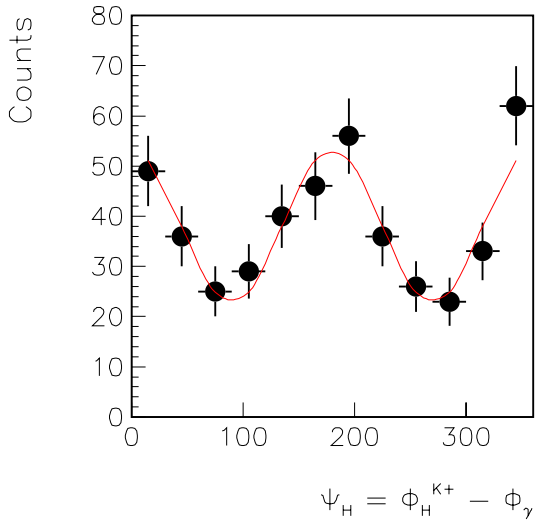

Figure 21: The distribution of azimuthal decay-angle of $K^+(\phi_K)$ relative to the photon polarization (Φ_γ) in the helicity system. The curve shows the result of fitting with the function of $(1 + A \times \cos 2(\phi_K - \Phi_K))$ where A is the fitting parameter.

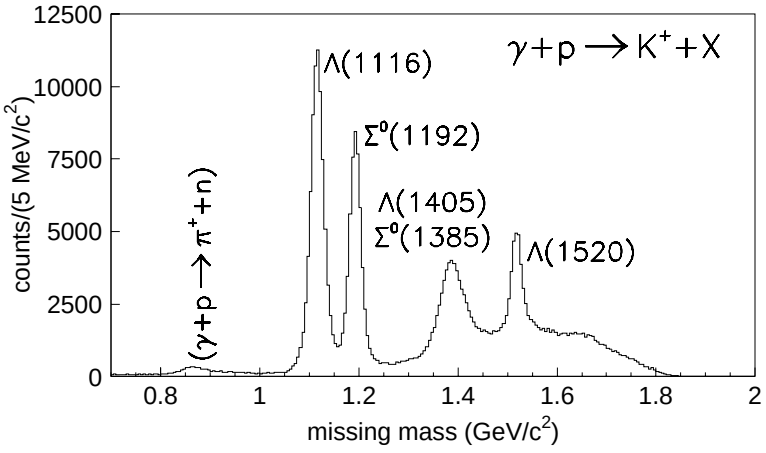

Figure 22: Missing-mass spectrum for the p(γ, K^+)X reaction.

polarization asymmetry distributions for Λ and Σ° productions. All the kinematical vari-

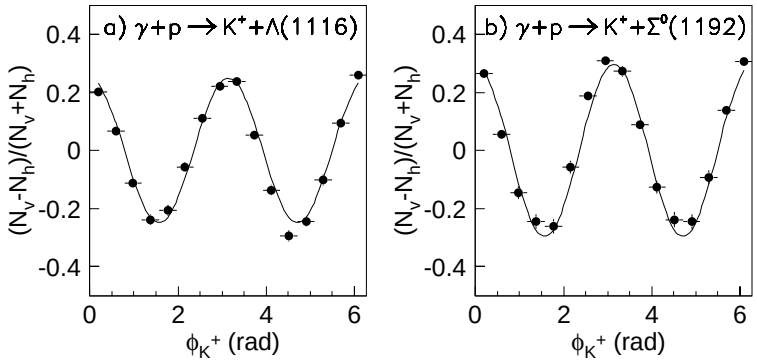

Figure 23: Asymmetries for the (a) p$(\gamma, K^+)\Lambda$ and (b) p$(\gamma, K^+)\Sigma^0$ reactions for all events. A fit to the data with $C \cos 2\phi$ is superimposed.

ables except for the K^+ polar angle were integrated over our acceptance region. Most of the acceptance effects were canceled by taking a ratio of $(H - V)/(H + V)$, where H and V are number of events in each angle bin for horizontal and vertical polarizations. We conclude that none of the existing theoretical calculations does not reproduce the measured photon polarization asymmetries for $\Lambda(1116)$ and $\Sigma^0(1192)$. In order to clarify the reaction mechanisms to produce Λ and Σ° via photoreactions, one can definitely say that more measurements for additional polarization observables are needed. The C_{BT} measurements for production of Λ and Σ° will provide us a smoking gun data for the complete understanding of the photoreaction mechanism from uud to uds quark systems, and the hadron structures.

6 Experimental consideration with HD target at SPring-8

In designing the experiment at SPring-8, we should consider the advantages of the present achievements at SPring-8, and the currently developed HD target in order to have a realistic path to perform the above-mentioned experiments within a reasonable time delay. One of the advantages at SPring-8 comes from the fact that we can use the fully-polarized photon beams in the energy range from 1.5 to 2.4 GeV. In addition, the detectors to be used have been already debugged in the preceding experiments. As advantages of the polarized HD target, we point out that the basic developments have been made to obtain independent and high polarizations of protons and deuterons, and that the background contribution from each other is rather low. We have a possibility to compare the data on polarized protons and on polarized neutrons in a model independent method (see Section 3.4).

The search for a signal in the double longitudinal asymmetry at forward angles seems to be very promising, because the incoming γ-ray knocks out a strange quark pairs in the nucleon, and produces a ϕ meson at forward angles as the final state. The goal here is to determine whether or not there is such a signal observed within $10-20\%$ precision accuracy. The reasonable run time of the experiment is the order of a month with a circularly polarized beam on longitudinally polarized protons in the HD target. Depending on the sensitivity of such an experiment, a systematic experimental program could be built, including also the program for polarized neutrons. As already mentioned, we have a great advantage of using the existing spectrometer to detect the ϕ meson decays which produce K^+ and K^-.

The verification of the GDH sum rule on neutron still stays a long standing problem. As described in Section 3.4, a polarized HD target is probably the only way to access accurate and model independent measurements of total cross sections on the "free" neutron. This experiment, requiring a 4π calorimeter, will be also performed with a high priority.

Since there still remain numerous open questions concerning the nucleon resonances study by photonic excitation, some specific double observables should be picked-up, according to their feasibility and their ability to discriminate among various models giving equivalent predictions for the previously measured observables.

Here it is necessary for us to discuss possible setups of ϕ photoproduction experiment with a polarized HD target at SPring-8. In the following sub-sections, we describe three different experimental designs:

- A setup with a HD target system, which is modified based on the GRAAL design, and is combined with the LEPS spectrometer. (Possibility 1)
- A setup with a large superconducting solenoidal magnet, which is placed at the outside of the nose structure of the HD target as a holding magnet. The LEPS spectrometer is used to analyze charged products. (Possibility 2)
- A setup with a time projection chamber, which is used as a spectrometer. The same HD target system as Possibility 1 is used. (Possibility 3)

In the last sub-section, we describe the beam-time estimation for the ϕ-meson production experiments.

6.1 Setup Possibility 1

To design the HD target, the field homogeneity of a holding magnet (a superconducting coil inside the nose structure) was checked. We studied the possibilities to use a superconducting coil with larger radii (R = 10 cm, 15 cm, 20 cm, 25 cm, 30 cm), by taking

into account the condition that charged particles accepted in the spectrometer should not hit the coil. The magnetic fields were simply calculated by using the Biot-Savart law for a coil with a certain radius and length. A current density was set to 1130 A/mm^2, and it was assumed that the coil consists of seven layers with 0.3 mm-diameter wires to get a maximum magnetic field of about 2 Tesla. (The magnetic field is needed to be larger than 1 Tesla to maintain polarization in the relaxation time of $\sim$10 days. Although confirmation is necessary, the relaxation time may be much enlarged by using a stronger field, and setups are considered with $\sim$2 Tesla below.) Fig. 24 shows the maximum magnetic field values with different coil shapes. Fig. 25 (Fig. 26) shows differences between maximum and minimum magnetic field in the HD target volume, the length of which was assumed to be 150 mm (200 mm). We find that when the radius is smaller than 25 cm and the length is longer than 50 cm, we can get the magnetic field higher than 2 Tesla. The field homogeneity with the 150 mm long target becomes within 3% level, while the homogeneity with the 200 mm long target is at 5% level for a reasonable coil length (600$\sim$700 mm). These coil geometry will be finally determined by considering also the available acceptance depending on a target z-position as described later.

The field inhomogeneity is also affected by the existence of the fringing field of the dipole magnet of the LEPS spectrometer. Fig. 27 shows the y-component distribution of the fringing field as a function of the z-position along the beam direction. At the position around -1200 mm, the homogeneity is $\sim$1% if we assume 2 Tesla of the holding field.

We have to set a HD target at a slightly upstream position if we take into account the size of a superconducting coil and the effect of the fringing field from the dipole magnet. Therefore, we studied the spectrometer acceptance as a function of a target z-position. Upper panels in Fig. 28 and 29 show a target position dependence of the relative acceptances of ϕ photoproduction events in the region of $t > -0.2$ (GeV/c^2)^2 and $t > -0.3$ (GeV/c^2)^2 with the same detector setup as those in the present LEPS experiments except for a target. For this purpose, simulation calculations in the Monte-Carlo method were carried out without considering decay-in-flight. Events with K^+ and K^- detections are only taken into account. Acceptances were normalized by those obtained with the 5 cm-long LH_2 target, which was set at $z = -945$ mm in the same way as the LEPS experiment (solid line in Fig. 28 and 29). The relative acceptance with the 15 cm-long LH_2 target (z = -995 mm) used recently is also shown in the figures. The acceptances drop significantly with departing from the present target position of $z = -945$ mm because of the limitations of the active areas of SVTX, AC and STC. Since it is rather difficult to move them to an upstream position due to a nose structure of the HD target system, sizes of those detectors were enlarged in the simulation calculations. The results are shown in the lower panels of Fig. 28 and 29. Now the spectrometer acceptances are limited by the size of DC3 (for $z > -1400$ mm) or DC1 (for $z < -1400$ mm), and higher acceptances

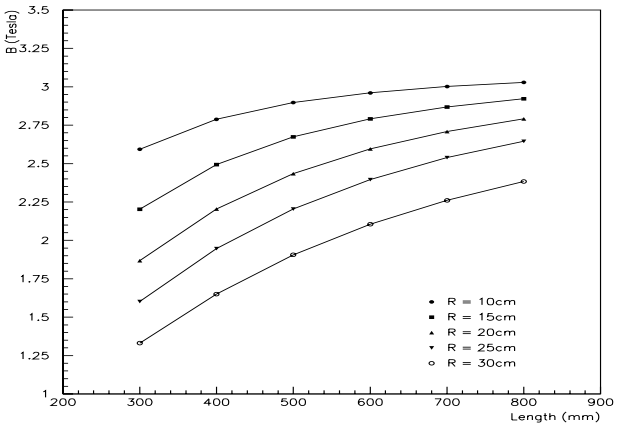

Figure 24: Maximum magnetic fields with various radii of a superconducting coil.

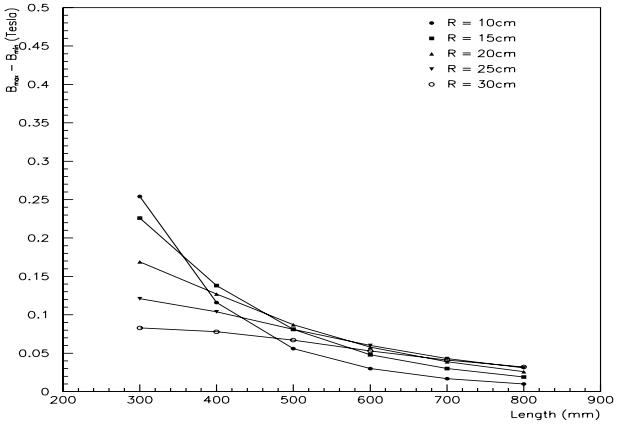

Figure 25: Field homogeneity in a 150mm-long target.

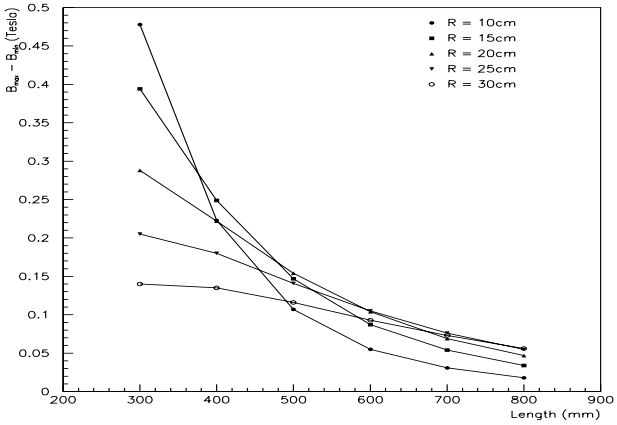

Figure 26: Field homogeneity in a 200mm-long target.

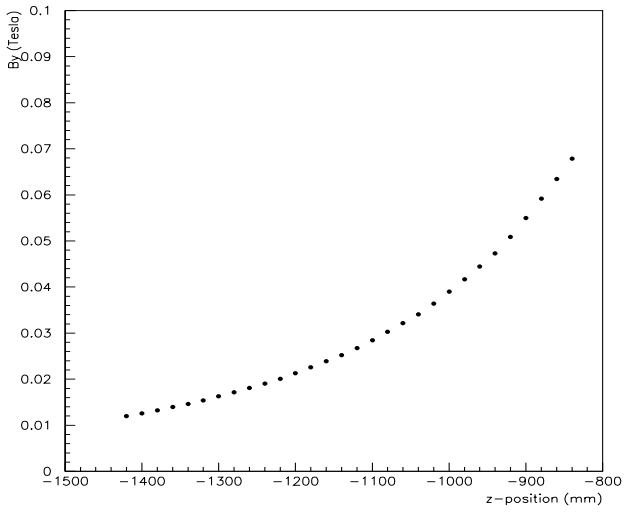

Figure 27: Fringing field distribution of the dipole magnet. The B_y components are plotted as a function of the z-position along the beam direction.

By taking into account the field homogeneity and the

z-dependence of acceptances, we can decide that one of possible solutions is to locate a 150 mm-long target at $z = -1300$ mm with a superconducting coil with a radius of 150 mm and a length of 600 mm. With this setup, the opening angles determined by the coil size are 21.8° - 33.7° depending on the z-position in the target volume. These angles are comparable to the current opening angles obtained for the 150 mm-long LH_2 target and the SVTX active area. The field homogeneity is expected to be less than 5% by taking into account the effect from both the holding field and the fringing field. The field homogeneity less that 5% is roughly needed to keep polarization. By assuming that a total magnetic field is a superposition of the fields from the superconducting coil and the dipole magnet, ϕ photoproduction events were again generated in the MC calculation with the setup mentioned above. K^+ tracks are azimuthally rotated in the superconducting coil typically by 10°. The spectrometer acceptances were comparable with those obtained in the case without the holding field within statistical errors.

Profiles of K^+ tracks (any t but only tracks reconstructible in the spectrometer) at SVTX, a nose end (assumed to $z = -900$ mm) and a coil end are expanded because the distance between the target and the spectrometer becomes longer. The active area of a tracking detector at the current SVTX position must be enlarged to the sizes of ± 300 mm and ± 150 mm in the x and y directions, respectively. The size of the IBC window at the nose end is needed to be ± 200 mm and ± 100 mm in the x and y directions, respectively. The designed radius of the coil is large enough.

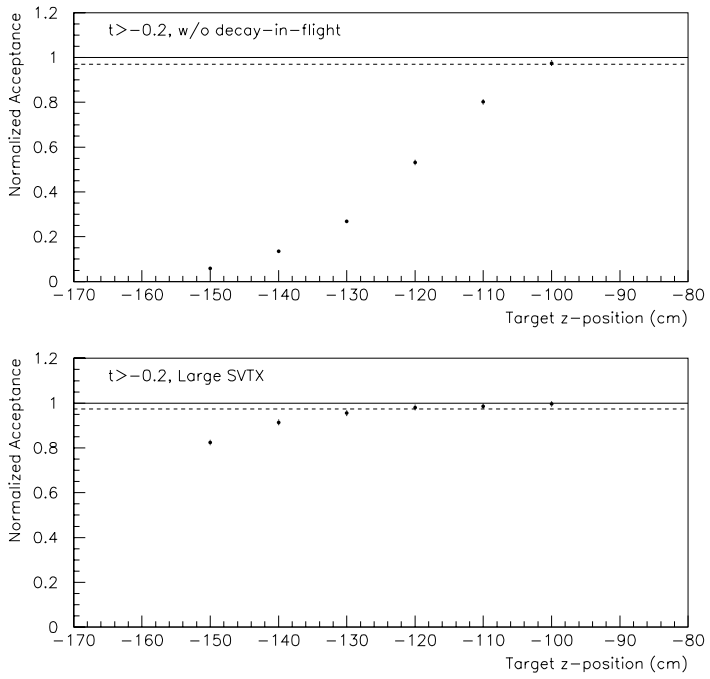

Figure 28: Z-dependences of spectrometer acceptances for ϕ photoproductions in the region of $t > -0.2$.

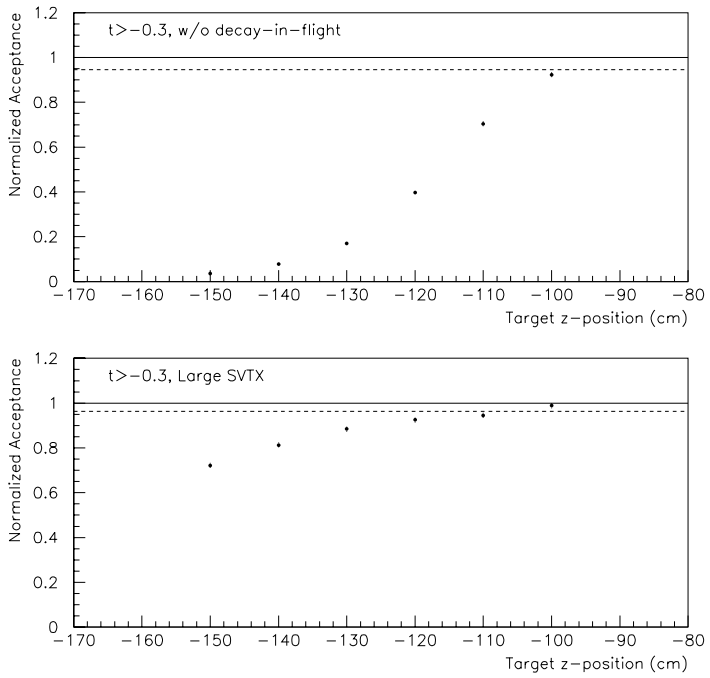

Figure 29: Z-dependences of spectrometer acceptances for ϕ photoproductions in the region of $t > -0.3$.

The HD target and the superconducting coil can be placed just under the main body of the "In-Beam" cryostat. This would be an advantage to get a higher cooling power.

6.2 Setup Possibility 2

The second possibility is to arrange the experiment with a large solenoidal coil, which will be placed at the outside of the nose structure and can be used as a holding magnet of the HD target system. A superconducting magnet with a radius of 30 cm and a length of 80 cm has been already prepared for a newly developed time projection chamber (TPC), which will be used for the nuclear target experiments to study the decay of $\Lambda(1405)$. In this solenoidal coil, the magnetic field of 2.5 Tesla has been obtained. The field homogeneity is 10^{-4} over the region $-25 < z < +25$ mm. Fig. 30 shows the distribution of the magnetic field measured along the z-axis (the central axis) by using a hole probe. The measured field homogeneity is less than 0.8% over the region of $-100 < z < +100$ mm.

The LEPS spectrometer will be used to analyze the charged particles from photoreactions. The acceptance of ϕ photoproduction events is described as a function of the z-position of the HD target in the same way as shown in Fig. 28 and 29. Since the length of the magnetic shield of the solenoidal coil is 100 cm and the length of the iron yoke of the dipole magnet is 60 cm, a HD target can be located at the same z-position (~ -950 mm) as used in the current experiment. The STC, AC and SVTX can be installed at the inside of the solenoidal coil. There is no need to enlarge them in this option. The radius of the nose part of the HD target system can be reduced in the range from 10 to 15 cm compared with those in the case of "Possibility 1", because a holding magnet is moved to the outside. Only one remained problem is the length of the nose part. This length should be in the range from 60 to 70 cm because of the length of the magnetic shield. It should be noted that although we have installed the HD target with a long nose with a sufficient cooling power in the GRAAL experiment, some additional work at SPring-8 may be needed because the radius of the nose will be enlarged than that in the GRAAL experiment.

6.3 Setup Possibility 3

An alternative option is to use the time projection chamber (TPC) as a spectrometer instead of the LEPS spectrometer. The TPC is now under development for nuclear target experiments. The TPC shape was assumed to be a thick tube structure with an inner diameter of 2.5 cm, an outer diameter of 54.62 cm and a length of 88.0 cm. All those parameters are close to the actual design. By using the compact TPC, the flight lengths for reconstructible kaons become short so that the acceptance loss due to the decay-in-

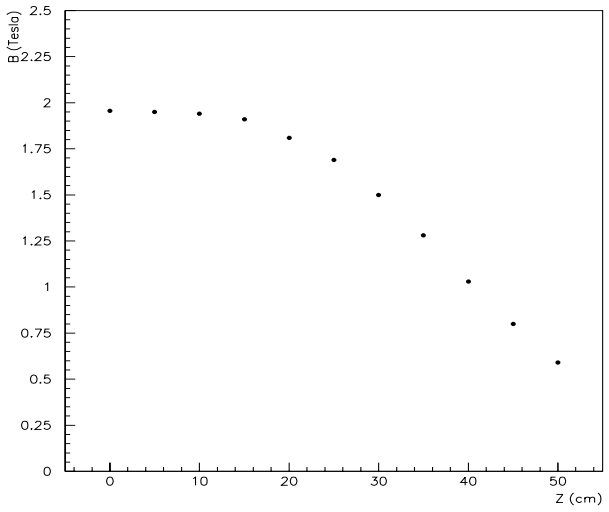

Figure 30: The magnetic field distribution along the central axis of the superconducting solenoid with a current of 58 A. The field strengths are plotted along the central axis (z-axis).

flight gets small.

In the acceptance studies, ϕ photoproduction events have been generated in the MC simulations. Events with two charged kaons are accepted if both the K^+K^- tracks pass through the TPC volume with a reconstructible flight length in the xy projection. The minimum flight length is estimated to be 3.45 cm by assuming that a track path is detected at least at the inner 5 cathode pads. Fig. 31 shows the relative acceptances as a function of the target z-positions for the cases with and without decay-in-flight. The acceptances are normalized by that calculated under the condition without decay-in-flight and with the LEPS spectrometer. The dashed straight line indicates a relative acceptance with decay-in-flight and with the LEPS spectrometer. It is unfair to directly compare the acceptances with the TPC and the LEPS spectrometer because the detail geometries and reconstruction efficiencies are unknown for the TPC. Obviously, there are advantages and disadvantages for both the cases; the resolution is excellent in the case of the spectrometer experiment, and the acceptance solid angle is large in the TPC experiment. It is evident that the event loss by decay-in-flight is greatly reduced in the case of using TPC.

Fig. 32 shows the distribution of the measured magnetic field along the z-direction which is produced in the solenoidal coil of the TPC. We have a field inhomogeneity of $\sim$2% at the position of $z = 1000$ mm (from the center of the TPC) for a holding field of the HD target if the field strength is assumed to be 2 Tesla. Consequently, a setup with the TPC and the HD target, which is located at 100-120 cm upstream of the TPC may

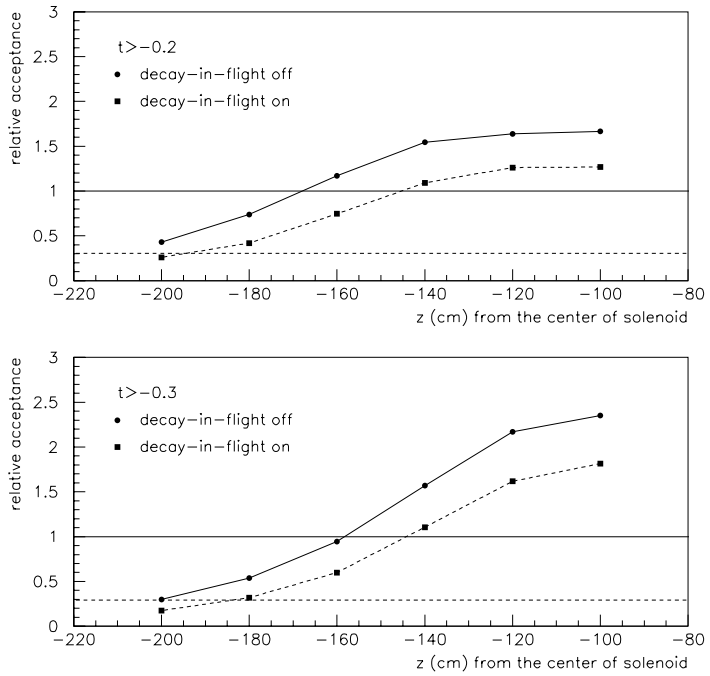

Figure 31: Z-dependences of the TPC acceptances for ϕ photoproductions in the region of t > -0.2 (upper) and t > -0.3 (lower).

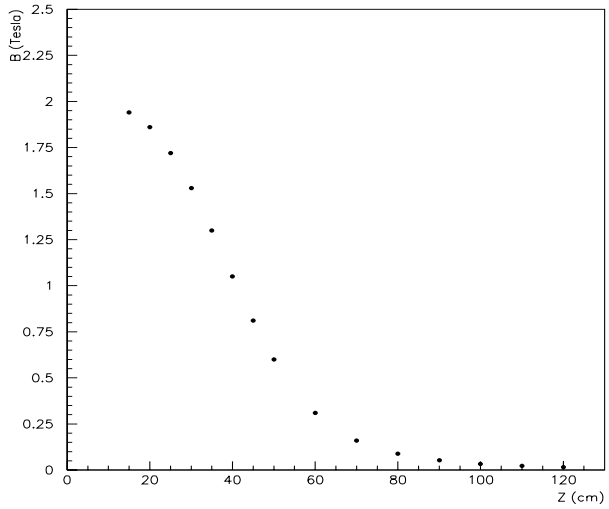

Figure 32: The magnetic field distribution of the superconducting solenoid with a current of 60 A. The field strengths are plotted along the central axis (z-axis).

give a much larger acceptance than those for a setup with the LEPS spectrometer. The same target design as "Possibility 1" can be used for this setup. Unknown factors, like a π/K separation, momentum resolutions and reconstruction efficiencies, should be taken into account in the further studies. (Particle identification will be done by dE/dx of a track, and 1σ separation of pion and kaon was expected for momentum lower than 0.7 GeV/c^2 based on a test experiment. The performance of the particle identification may reduce acceptances in the case of the TPC.)

6.4 Estimations for Experiment

A main subject of the proposed experiment is a measurement of beam-target asymmetry of ϕ photoproduction from a polarized proton. The beam-target asymmetry (C_{BT}) is calculated by

$$C_{BT} = \frac{(\sigma_P - \sigma_{BG}) - (\sigma_A - \sigma_{BG})}{(\sigma_P - \sigma_{BG}) + (\sigma_A - \sigma_{BG})} = \frac{\sigma_P - \sigma_A}{\sigma_P + \sigma_A - 2\sigma_{BG}}, \tag{12}$$

where σ_P (σ_A) represents the spin parallel (anti-parallel) cross section from a HD target and σ_{BG} describes a common background contribution mainly from an unpolarized deuteron. Since three measurements of σ_P, σ_A and σ_{BG} will be independent, an error on the beam-target asymmetry (ΔC_{BT}) is written to be

$$\begin{aligned}\frac{(\Delta C_{BT})^2}{C_{BT}^2} &= \frac{4(\sigma_A - \sigma_{BG})^2}{(\sigma_P - \sigma_A)^2(\sigma_P + \sigma_A - 2\sigma_{BG})^2}(\Delta\sigma_P)^2 + \\ &\quad \frac{4(\sigma_{BG} - \sigma_P)^2}{(\sigma_P - \sigma_A)^2(\sigma_P + \sigma_A - 2\sigma_{BG})^2}(\Delta\sigma_A)^2 + \\ &\quad \frac{4}{(\sigma_P + \sigma_A - 2\sigma_{BG})^2}(\Delta\sigma_{BG})^2. \end{aligned} \tag{13}$$

Defining the ratio R= $\frac{\sigma_{BG}}{(\sigma_P+\sigma_A)/2}$ using the background cross section σ_{BG} and an averaged cross section $(\sigma_P+\sigma_A)/2$, we obtain a relation between σ_P and σ_A as $\sigma_A = \frac{1-C_{BT}(1-R)}{1+C_{BT}(1-R)}\sigma_P$. If it is assumed that σ_P and σ_A will be measured with the same precision, $\Delta\sigma_A$ is written as $\frac{1-C_{BT}(1-R)}{1+C_{BT}(1-R)} \cdot \Delta\sigma_P$. By using these relations, the following equation is obtained:

$$\frac{(\Delta C_{BT})^2}{C_{BT}^2} = \frac{\{1 - C_{BT}^2(1-R)\}^2 + C_{BT}^2R^2}{2C_{BT}^2(1-R)^2} \cdot \frac{(\Delta\sigma_P)^2}{\sigma_P^2} + \frac{R^2}{(1-R)^2} \cdot \frac{(\Delta\sigma_{BG})^2}{\sigma_{BG}^2}. \tag{14}$$

Titov suggested that 1% of strange quark contents would produce $C_{BT} = 0.3$ in a small $|t|$ region. The fraction R depends not only on coherent and incoherent cross sections from deuteron but on an offline cut for a missing mass of K^+ and K^- tracks, which will be affected by Fermi motion in deuteron. If R is assumed to be 0.5, Eqn. 14 is rewritten as $\frac{(\Delta C_{BT})^2}{C_{BT}^2} = 20.8 \cdot \frac{(\Delta\sigma_P)^2}{\sigma_P^2} + 1.0 \cdot \frac{(\Delta\sigma_{BG})^2}{\sigma_{BG}^2}$. This means that 10% (20%) precision of C_{BT}

requires 2.2% (4.4%) measurement of σ_P, for example, by neglecting the second term. If only statistical error is taken into account, ∼2000 (∼500) events of ϕ photoproductions has to be collected for the successful measurement.

In the LEPS experiment from December 2000 to June 2001, we collected about 3000 events of ϕ photoproductions in a K^+ and K^- detection mode by using a 5 cm-long LH_2 target. This yield corresponds to the production rate per photon of $\sim 1 \times 10^{-9}$. (There were other experiments in the period from 2000 to June 2001, and of course the accelerator was not always operated because of its scheduled shutdown for maintenance. Photon beam intensity was also low in the beginning of the period.) About half of the events are clarified to belong to the region of $t > -0.2$. Assuming a 15 cm-long HD target, $R = 0.5$ and 0.8×10^6 photons per second, ∼100 events of ϕ productions would be collected for $t > -0.2$ in one day. A collection of 2000×2 events (500×2 events), which corresponds to the 10% (20%) accuracy measurement for C_{BT}, would be achievable in the 40 days (10 days) run time. Fig. 33 shows an expected precision of a beam-target asymmetry measurement as a function of the experimental period. The beam time with 10-40 days will be achievable with present technologies for the HD target.

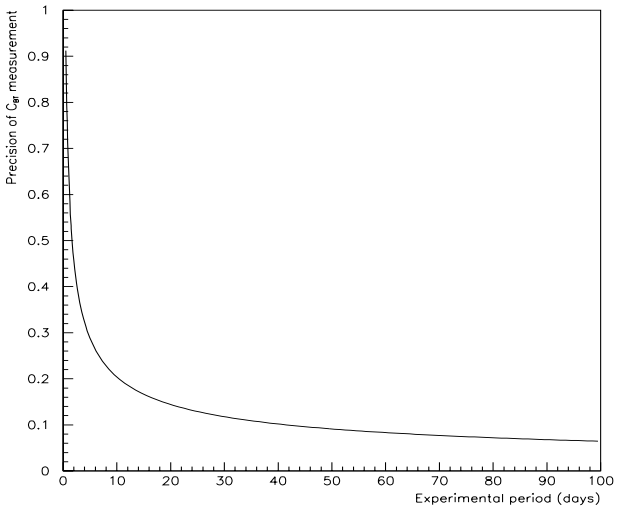

Figure 33: Expected precision for the beam-target asymmetry measurement as a function of the experimental period.

7 Estimation of the costs for fabrication and installation

Table 2 lists all the costs including the employment fee for developing, installing the HD target and for performing the experiments.

The total cost for the construction of the polarized HD target system is estimated to be about 3 million US$, most of which are for dilution refrigerator equipped with a high field superconducting coil (750 k US$), in-beam cryostat (700 k US$), storage cryostat (150 k US$), building (390 k US$), and HD gas (150 k US$).

As the first stage of the HD target development, we start to clean up the existing building for the cryogenic system. 20 years ago, this building was used to produce liquid He for the superconducting solenoid magnet to rotate the spin of the 65 MeV proton beam for the polarization experiments. But, the equipment became old now and it is not used for about 15 years. The building is almost empty, and used now for only a tiny experiment. This building is very suitable for our purpose to produce the HD target at RCNP. However, the influstructure such as the power line and air conditioning system should be improved to fit to the aim of the HD target production. This is also officially good since the building is not used in the correct political way for the cryogenic purposes for a long time. Fortunately, it has been decided at RCNP that this building will be clean up firstly in this fiscal year 2003.

In a paralel way, the HD target development is continued at ORSAY in 2003. We plan to have the actual construction phase in 2004. The HD production facility will be constructed in 2004. Since there are many parts which are necessary to be developed at the RCNP side, we start the developments of small devices such as the NMR system with a small money in 2004. Obviously, we come to the actual designing phase for the installation of the HD target in 2003.

8 Time schedule

We summarize the time schedule for developing the HD target and for installing it at SPring-8 in Table 3. Among all the equipments necessary to produce and exploit polarized HD, the key one is the Dilution Refrigerator equipped with a high field superconducting coil. This type of equipment is commercially available and can be delivered within one year after order. The production of the polarized HD target is now not a big problem, if we consider the recent technology developments; i) one can follows the protocol which is now rather well established by numerous polarization runs at Brookhaven and Orsay, ii) one uses good quality double distilled HD gas, for which distillation apparatus already exists and its performance is checked.

So far, we did not decide what kinds of IBC will be optimal to perform the best experiments at SPring-8. In the case of the present LEGS and GRAAL IBC, we use an old technology based on liquid ^{4}He and ^{3}He pumped baths, and the devices can be cooled down till 1.5K and 0.5K, respectively. They consume a significant (prohibitive) amount of ^4He, necessary to provide the cold source. A possible improvement would be

Table 2: Cost estimation

Item	cost (K US$)
Dilution fridge + Coil	750
building	390
Storage Cryostat	150
IBC (1st. generation)	100
IBC (2nd. generation)	200
IBC (3rd. generation)	400
Transfer Cryostat 1	50
Transfer Cryostat. 2	50
Frame	50
NMR system $\times$ 2	30 $\times$ 2
others	20
50 moles HD gas	150
HD distillation apparatus	30
Residual gas analyzer	30
Helium cost	30
(production)	(20)
(running)	(10)
Power line and electric and mechanical parts etc. at RCNP	150
Power line etc at Spring-8	150
Employment fee for scientists	100
Total	2,710

to use a cryogenerator for the cold source. This improvement is under study at Orsay; it increases the original cost significantly, but the savings in liquid ^4He is enormous. Another approach would be to use a small dilution unit, in order to reach temperatures below 0.5K, which is extremely attractive in view of the increase of relaxation times at lower temperatures. Such an approach has been chosen by the LSC, and will be tested during the year 2003. It seems obvious that the SPring-8 IBC will be fabricated in a sophisticated way by taking into account all the lessons which will be learned during the coming year both in US and in France. Therefore, the best choice will be clear shortly, allowing the development of the best IBC for SPring-8 in parallel with the construction of the DR.

The TC and SC are more conventional cryogenic devices and it will be sufficient to correct the previous few misconceptions. The argumentation developed here shows that within a delay of 3 years, one can dream of an experiment performed at SPring-8.

9 Conclusions

We propose to construct a polarized HD target for photoproduction experiments at LEPS facility at SPring-8, where a polarized photon beam is available in the energy region from 1.5 to 2.4 GeV. We aim to perform the experiment of ϕ photoproduction off a nucleon at forward angles as a main physics. Measurement of the double polarization asymmetries for the ϕ photoproduction with the polarized target and the circularly polarized photon beam enables us to investigate small and exotic amplitudes via the interference with dominant amplitudes. We can study the interesting subjects such as the $s\bar{s}$-quark content of nucleons, which is currently considered to be non-negligible. A measurement of a beam-target asymmetry at small $|t|$ (forward angles) with a $1.5 - 2.4$ GeV photon beam is promising to extract a small component via a large interference effect by comparing with other competitors. Other subjects in hadron physics, such as the missing baryon resonances, the GDH sum rule and so on, can be also accessible in a clear method via the polarization observables by using the HD target.

Since the cross section of the ϕ photoproduction is not very large, the target should not contain heavy elements generating huge amounts of backgrounds. The HD target is an ideal polarized target because it consists of hydrogen and deuterium, which are necessary for investigating the $s\bar{s}$-quark content of both proton and neutron. A contribution from a small amount of aluminum will be subtracted easily. The technology for the polarized HD target has been developed with longstanding great efforts by the Syracuse, BNL and ORSAY groups. Now we are reaching at the final stage to apply the polarized HD target for actual experiments at LEGS and GRAAL. Protons with spin 1/2 and deuterons with spin 1 are polarized independently, and are independently reversible. Hydrogen

Table 3: Time Schedule for Polarized HD target

2003	2004	2005	2006	2007
ORSAY and GRAAL				
1. Production of polarized HD at ORSAY. 2. Experiment at GRAAL. 3. Improvement of the HD target. 4. Study of relaxation time with various conditions.	1. GDH sum rule experiment. 2. Distillation of HD gas. 3. Application.	1. Distillation of HD for LEPS target.	1. Distillation of HD for LEPS target.	Not scheduled.
RCNP and LEPS/SPring-8				
1. Preparation of HD target production building at RCNP.	1. Construction of the HD production facility at RCNP. 2. Development of NMR system.	1. Installation of storage cryostat and transfer cryostat at RCNP. 2. Installation of IBC at SPring-8.	1. Production of polarized HD. 2. Installation of HD target to IBC at SPring-8. 3. Experiment at LEPS/SPring-8.	(Continued) 1. Production of polarized HD. 2. Experiment at LEPS/SPring-8.

and deuterium vector polarization, exceeding 95% and 70% respectively, are attainable with recent technology developments for the HD target handling in low temperature and high magnetic field. Solid polarized HD samples are kept in the frozen-spin conditions for temperatures below 4 K at a moderate holding fields (0.5 T), which allows easy transportation. The polarization production site can be separated from the experimental one. For example, the polarization is produced at RCNP of Osaka University, and the HD target is transported to SPring-8 and used for the experiment at LEPS. Relaxation times longer than a week for H and longer than a month for D can be expected at 0.5 K and 0.5 T, which is enough to perform experiments using a rather simple in-beam cryostat (IBC). By introducing a sophisticated IBC with a better condition of lower temperature and higher magnetic field, relaxation times are expected to be longer.

We estimate that it takes about 4 years to construct the polarized HD target. Time schedule for the construction is as follows;

1. 1st year: Preparation of a building for the HD target production at RCNP.
2. 2nd year: Construction of the HD production facility at RCNP. Development of NMR system.
3. 3rd year: Installation of storage cryostat and transfer cryostat at RCNP. Installation of in-beam cryostat at SPring-8.
4. 4th year: Production of polarized HD. Installation of the HD target to in-beam cryostat at SPring-8. Experiment at LEPS at SPring-8.

The estimated yield for the ϕ photoproduction from the HD target at $t > -0.2$ (GeV^2) is about 100 events/day for each helicity if the target length is assumed to be 15 cm. If the beam-target asymmetry from a proton is assumed to be 0.3, which would be produced with 1% of $s\bar{s}$ content in the LEPS photon energy at forward angles, a measurement with 20 % (10 %) precision will be achieved in 10 days (40 days). The accuracy is enough to determine an $s\bar{s}$-quark admixture in the proton and the estimated beam time is reasonable for the first experiment using the polarized HD target.

References

[1] J. Ashman *et al.* [European Muon Collaboration], Phys. Lett. B **206**, 364 (1988).

[2] D. Adams *et al.* [Spin Muon Collaboration (SMC)], Phys. Lett. B **329**, 399 (1994)

[3] K. Abe *et al.* [E143 Collaboration], Phys. Rev. Lett. **74**, 346 (1995).

[4] L. A. Ahrens *et al.*, Phys. Rev. D **35**, 785 (1987).

[5] J. F. Donoghue and C. R. Nappi, Phys. Lett. B **168**, 105 (1986).

[6] J. Gasser, H. Leutwyler and M. E. Sainio, Phys. Lett. B **253**, 252 (1991).

[7] J. Reifenroether *et al.* [ASTERIX Collaboration], Phys. Lett. B **267**, 299 (1991).

[8] C. Amsler *et al.* [Crystal Barrel Collaboration], Phys. Lett. B **346**, 363 (1995).

[9] A. Bertin *et al.* [OBELIX Collaboration], Phys. Lett. B **388**, 450 (1996) [arXiv:hep-ex/9607006].

[10] S. Okubo, Phys. Lett. **5**, 165 (1963).

[11] A.I. Titov and T-S.H. Lee, Phys. Rev. C **66**, 015204 (2002).

[12] A.I. Titov, T.-S. H. Lee, H. Toki, and O. Streltsova, Phys. Rev. C **60**, 035205 (1999).

[13] E.M. Henley, G. Krein, and A.G. Williams, Phys. Lett. B **281**, 178 (1992); E.M. Henley, T. Frederico, S.J. Pollock, S. Ying, G. Krein, and A.G. Williams, Few-Body Syst. (Suppl) **6**, 66 (1992).

[14] A. I. Titov, Y. Oh, and S. N. Yang, Phys. Rev. Lett. **79**, 1634 (1997).

[15] A.I. Titov, Y. Oh, S.N. Yang, and T. Morii, Phys. Rev. C **58**, 2429 (1998); Nucl. Phys. A **684**, 354 (2001).

[16] A. Airapetian *et al.* [HERMES Collaboration], arXiv:hep-ex/0302012.

[17] H.J. Besch, G. Hartmann, R. Kose, F.Krautschneider, W. Paul, and U. Trinks, Nucl. Phys. B **70**, 257 (1974).

[18] A.I. Titov, M. Fujiwara and T-S.H. Lee, Phys. Rev. C **66**, 0222202 (2002).

[19] Y. Oh. A.I. Titov and T.-S. H. Lee, Phys. Rev. C 63, 025201 (2001).

[20] M. Battaglieri *et al.,* Phys. Rev. Lett. **90**, 022002 (2003).

[21] S.B. Gerasimov, Sov. J. Nucl. Phys. **2**, 430 (1966).

[22] S.D. Drell and A.C. Hearn, Phys. Rev. Lett. **16**, 908 (1966).

[23] M. Hosoda and K. Yamamoto, Prog. Theo. Phys. **36**, 425 (1966).

[24] J. Ahrens *et al.,* Phys. Rev. Lett. **84**, 5950 (2000).

[25] J. Ahrens *et al.,* Phys. Rev. Lett. 87, 022003 (2001).

[26] Proceedings of the Symposium on the Gerasimov-Drell-Hearn Sum Rule and the Nucleon Spin Structure in the Resonance Region, Mainz, Germany, 14-17 June 2000, edited by D. Drechsel and L. Taitor.

[27] A.M. Sandorfi, C.S. Whisnant and M. Khandaker, Phys. Rev. D **50**, R6681 (1994).

[28] L. Tiator, D. Drechsel and S.S. Kamalov, *Proceedings of the NSTAR2000 Conference "Excited Nucleons and Hadronic Structure", Newport News, USA, February 2000, p 343.* World Scientific, Ed. V. D. Burkert, L. Elouadrhiri, J. J. Kelly and R. C. Minehart.

[29] D. Drechsel, Prog. Part. Nucl. Phys. **34** (1995) 181.

[30] A. M. Sandorfi, in Proceedings of FRONTIER96, edited by H. Toki, T. Kishimoto and M. Fujiwara, World Scientific, March 7-9, 1996, pp. 17.

[31] T. Iwata, in Proceedings of the International Symposium on the Electromagnetic Interactions in Nuclear and Hardon Physics, Osaka, Japan, 4-7 December, 2001 eds. M. Fujiwara and T. Shima, World Scientific, pp. 578.

[32] M. Gell-Mann, M. Goldberger, and W. Thirring, Phys. Rev. **96**, 1612 (1954).

[33] C. Bennhold, private communications.

[34] A. Honig *et al.*, Nucl. Instr. and Meth. in Phys. Research, **356** (1995) 39.

[35] J.-P. Didelez, Nuclear Physics News, Vol 4, N^0 3 (1994) 10.

[36] A. Honig *et al.*, "Spin96", Proceedings of the 12th Int. Symp. on High-Energy Spin Physics, Amsterdam Sept. 1996, edited by C.W. de Jager et al., in "World Scientific", p. 365.

[37] M. Breuer *et al.*, "Spin96", Proceedings of the 12th Int. Symp. on High-Energy Spin Physics, Amsterdam Sept. 1996, edited by C.W. de Jager *et al.*, in "World Scientific", p. 272.

[38] A. Honig, Phys. Rev. Lett. **19**, 1009 (1967).

[39] R.S. Rubins, A. Feldman, and A. Honig, Bull. Am. Phys. Soc. **11** (1966) 907.

[40] A. Honig and H. Mano, Phys. Rev., **14** (1976) 1858.

[41] G. Rouille *et al.,* Nucl. Instr. and Meth. in Phys. Research A **464**, 428 (2001).

[42] C. Commeaux *et al.* Proceedings of the 9th Seminar: Electromagnetic Interactions of Nuclei at Low and Medium Energies, Moscow, September 2000, pp 281.

[43] S. Whisnant *et al.,* in Proceedings of the International Symposium on the Electromagnetic Interactions in Nuclear and Hardon Physics, Osaka, Japan, 4-7 December, 2001 eds. M. Fujiwara and T. Shima, World Scientific, pp. 135.

[44] P. Gara (IPN, ORSAY), private communication.

[45] A. Braghieri, "Helicity dependence of exclusive pion photoproduction in the first and second resonance region", *GDH2002 Conference.*

[46] P. Grabmayr, "Experimental results for the GDH sum rule on the proton from pion threshold to 3 GeV", *GDH2002 Conference.*

[47] G. Cates, "Neutron spin structure study at Jefferson Lab Hall A", *GDH2002 Conference.*

[48] T. Hemmert, "Moments of spin-structure functions at small momentum transfer and the generalized GDH sum rule", *GDH2002 Conference.*

[49] "Measurement of the total photoabsorption cross section on the proton in 600 - 1500 MeV energy region at GRAAL", *In preparation.*

[50] F. Renard *et al.*, Phys. Lett. **B 528**, 215 (2002).

[51] O. Bartalini *et al.*, Phys. Lett. **B 544**, 113 (2002).

[52] F. Renard, PhD Thesis, Grenoble (1999).

[53] P. Hoffmann-Rothe *et al.*, Phys. Rev. Lett. **78**, 4697 (1997).

[54] A.I. L'vov, (private communication).

[55] Y. Sugaya and M. Nomachi, Nucl. Inst. and Meth. in Phys. Res. A **437**, 68 (1999).

[56] Y. Sugaya *et al.,* IEEE Trans. Nucl. Sci. **48**, 1282 (2001).

[57] J.K. Ahn, K. Imai (Spokespersons), *et al.*, LEPS/SPring-8 proposal Q014 (2002).

[58] M. Niiyama, *et al.*, PaNic02 proceedings (2003).

[59] T. Iwata (Spokesperson), *et al.*, LEPS/SPring-8 proposal (2001)

[60] S. Ishimoto *et al.*, J. Appl. Phys., 28(1989) 1963.

[61] J.J. Sakurai, Ann. Phys. 11, 1 (1960); J.J. Sakurai, Phys. Rev. Lett. 22, 981 (1969).

[62] T.H. Bauer *et al.*, Rev. Mod. Phys. 50, 261 (1978).

[63] A. Donnachie and P.V. Landshoff, Nucl. Phys. B267, 690 (1986).

[64] M.A. Pichowsky and T.-S. H. Lee, Phys. Rev. D56, 1644 (1997).

[65] T. Nakano and H. Toki, in Proc. of Intern. Workshop on Exciting Physics with New Accelerator Facilities, SPring–8, Hyogo, 1997, World Scientific Publishing Co. Pte. Ltd., 1998, p.48.

[66] A.I. Titov, Y. Oh, and S.N. Yang, Phys. Rev. Lett. 79, 1634 (1997);
A.I. Titov, Y. Oh, and S.N. Yang, Phys. Rev. C58, 2429 (1998).

[67] M.Q. Tran *et al.*, Phys. Lett. B 445, 20 (1998).

[68] T. Mart and C. Bennhold, Phys. Rev. C61, (R)012201 (2000).

[69] S. Capstick and W. Roberts, Phys. Rev. D58, 074011 (1998).

[70] A. d'Angelo, a talk in Baryons 2002 conference.

[71] N. Kaiser, P. B. Siegel and W. Weise, Nucl. Phys. A **594**, 325 (1995)

[72] J. C. Nacher, E. Oset, H. Toki and A. Ramos, Phys. Lett. B **455**, 55 (1999)

[73] T. Nakano, *et al.*, hep-ex/0301020

[74] R. G. Zegers *et al.* [LEPS Collaboration], arXiv:nucl-ex/0302005.